Nanotechnology for Environmental Engineering (2024) 9:389–409
https://doi.org/10.1007/s41204-024-00373-w

CRITICAL REVIEWS

Recent advances in remediating organic-laden wastewater using graphene-based nanomaterials

Olayinka O. Oluwasina[1] · Adedeji A. Adelodun[1,2]

Received: 3 April 2023 / Accepted: 10 May 2024 / Published online: 27 May 2024

Abstract

Due to their unique adsorptive potentials, graphene-based nano-composites [especially graphene oxide (GO)] have been recently researched intensively for sequestrating organic pollutants, such as dyes and pharmaceuticals. These pollutants are primarily adsorbed via π–π, H-bond, and electrostatic interactions, achieving 37–1148 mg g^{-1} maximum adsorption capacities. This review identifies the influence of pH, temperature, sorbate concentration, and sorbent dosage on the sorbate-sorbent interface. The investigated adsorptions occurred within pH 2–12, promoting cationic surfaces that achieved up to 394.6 mg g^{-1}. Also, both dyes and pharmaceuticals were predominantly removed endothermically (≥ 532.6 mg g^{-1}) than exothermically (≥ 14.10 mg g^{-1}). Further reusability tests over 3–15 cycles accomplished between > 50 and 100% removal efficiencies. In comparison, zeolites were other adsorbents with similar performances to functionalized GO, except that GO exhibits superior affordability, mechanical strength, specificity, and reusability. However, simultaneous removal of dyes and pharmaceuticals using GO requires further research for improved performance.

Keywords Dyes · Pharmaceuticals · Surface chemistry · Adsorption · Graphene oxide

Introduction

Environmental pollutants, particularly organics, threaten the global ecosystem and human health incessantly. For example, anthropogenic-based organics (dyes, insecticides, pharmaceuticals, and cosmetics) have been reportedly found in various surface and subsurface water bodies globally [1]. Specifically, fresh water is a necessity for life. However, its availability is consistently dwindling because of the continuous surface water contamination from improper waste disposal into rivers from sewages and wastewater treatment practices [2]. As a result, oral consumption of such contaminated water has been attributed to many severe diseases, such as diarrhea, cholera, dysentery, typhoid, and polio, causing approximately 485,000 diarrhea-based deaths annually [3].

For instance, pharmaceutical industries often require large quantities of water for routine operations, generating enormous amounts of wastewater. According to standard regulations, such wastewaters are filtered for nitrates, phosphates, and carbons before eventually discharging the effluents into water bodies. Still, some unwanted toxic metals, solids, and organics are residual in the effluents [4]. As a result, pharmaceutical wastewater could contain various organic pollutants, poisons, and minerals that could end up in drinking water supplies.

To mitigate against these environmental maladies, various pollution prevention and aftermath control techniques have been deployed, including oxidation [5], photocatalysis [6], filtration [7], precipitation [8], sedimentation [9], coagulation [10], osmosis [11], distillation [12], adsorption [13], and so on. However, these methods have inherent limitations, such as limited efficiency, high specificity, high-cost requirements, secondary waste generation, etc. [14, 15]. Therefore, a viable, efficient, low-cost, and easily accessible treatment technique critical for sustainable treatment amidst rapid technological advancement, population explosion, mechanized agriculture, and industrialization [16].

✉ Adedeji A. Adelodun
aaadelodun@futa.edu.ng; aaa@chem.ku.dk

[1] Department of Marine Science and Technology, The Federal University of Technology, P.M.B. 704, Akure 340110, Nigeria

[2] Department of Chemistry, University of Copenhagen, Universitetsparken 5, 2100 Copenhagen, Denmark

Background information on graphene and graphene oxide

Of the many mitigation options, adsorption is arguably the most popular and reliable for water detoxification [17] because of its ease-of-operation conditions, numerous adsorbent options, relative affordability, large-scale applicability, regeneration and reusability, ready functionalization, high efficiency, and designability [18, 19]. Specifically, graphene-based nanomaterials are excellent adsorbents for mitigating numerous environmentally hazardous compounds [20–23]. Carbon nanotubes (CNTs), graphene, and other carbon-based composite materials are advanced nanomaterials with high water purification performances [24]. Preparing graphene-based nano-composites has emerged as the most vital cutting-edge research in water purification. However, these materials are expensive, making them (and CNT materials) unsustainable and unrealistic for water purification. Still, they serve as the foundation for next-generation water purification materials with much-improved performance and flexibility [25].

Graphene, a two-dimensional (2D), one-atom-thick nanomaterial made of sp^2-hybridized carbon, has piqued immense research interest due to its impressive properties, such as high specific surface area (2600 $m^2\ g^{-1}$) [26], excellent thermal conductivity (5000 $W\ m^{-1}\ K^{-1}$) [27], high-speed electron mobility (200,000 $cm^2\ V^{-1}\ s^{-1}$ at room temperature) [28], high stiffness and strength (a 1000 GPa Young's modulus and 130 GPa break strength) [29], electrocatalytic activity [30], and excellent optical properties [31]. Graphene's applications are diverse, with enormous interest in medical, chemical, and industrial uses. Its inherent properties enable the fabricating of lightweight, thin, flexible, and strong display screens, electric/photonics circuits, optical electronics, photovoltaic cells, solar cells for energy storage, and ultrafiltration in water treatment. [32–35]. Based on this concept, diverse graphene derivatives have been prooduced and applied to environmental protection and detection. Intense efforts are directed at developing efficient yet affordable processes for fabricating graphene derivatives [such as graphene oxide (GO)] and reducing their expensive and somewhat difficult production procedures.

Graphene oxide is a precursor for producing single-layer graphene. It is composed of a single sheet layer of graphite oxide, which is synthesized by the chemical oxidation of graphite [36, 37]. Since it is hydrophilic, it effortlessly exfoliates and disperses in water or organic solvents [38, 39]. Oxygen-containing functional groups (such as carboxylic, epoxide, and hydroxyl groups), high surface area, and hydrophilicity make GO flakes an excellent prospective sorbent material [40, 41]. It exhibits a large adsorption capacity due to the large surface area [42–44]. The hydrophilicity of oxidized graphite allows water to be absorbed into the layered structure, further increasing the gap between the layers to 1.15 nm [45].

Graphene oxide is a yellow, oxidized solid with the same layer structure as graphite. Still, it has numerous irregular spacing arising from many oxygen-containing groups on the basal planes and sheep edges [46, 47]. Because of its high dispersivity (solubility) in water after oxidation, GO's propensity for removing water pollutants is superior to graphene's. Graphene oxide exhibits improved selectivity (adsorption and detection) while preventing aggregation where necessary. Here, we present compiled data from recent graphene-based nanomaterials for cleaning organic-laden wastewater from various industries. The adsorption mechanism, limiting factors, preferential adsorption, and effective surface area are estimated.

Organic pollutants in wastewater

Pharmaceuticals

Prescription and over-the-counter medicinal and veterinary drugs contain synthetic or natural chemicals with pharmacological effects [48, 49]. The present age in the pharmaceutical industry began with local apothecaries, expanding from their traditional role of dispensing botanical drugs (such as morphine and quinine) to wholesale manufacture in the mid-1800s, courtesy of the advent of applied research. For the first time, German pharmacist assistant Friedrich Sertürner isolated morphine, an analgesic and sleep-inducing chemical, from opium between 1803 and 1805. He named the substance after the Greek god of dreams, Morpheus [50]. Later, in the 1880s, German dye makers mastered the purification of individual organic compounds derived from tar and other mineral sources and developed primitive organic chemical synthesis procedures [51]. Improving the chemical synthetic methods allows scientists to systematically vary chemical substances' structures. As pharmacology grew, it broadened scientists' ability to assess the biological effects of these structural changes.

Approximately 10,000 pharmaceuticals with about 3000 components are licensed for animal and human treatments [52]. For instance, pharmaceutical consumption in European countries has climbed steadily from 2000 to 2015 due to rising cholesterol-lowering medications [53]. Antibiotics, analgesics, antipyretics, antidepressants, and chemotherapy chemicals are the most common constituents of pharmaceutical waste. Specifically, estrone, ethinylestrone, estradiol, and other pharmaceuticals are highly carcinogenic, while tetracycline is a recognized antibiotic that poses significant adverse effects on human health. Also, indiscriminate

environmental discharge of persistent antibiotics (such as chloramphenicol and sulphonamides) is a severe problem. Pharmaceutical concentrations in the aquatic environment have grown proportionally (from ng L^{-1} to mg L^{-1}) to the consumption trend [54, 55]. Tracking their environmental fate is highly tedious, given their widely dispersed variations. As a result, a priority list was produced that ranks the value of drugs based on influential factors, such as intake, toxicity, and persistence [56]. Figure 1 reveals the major release pathways of pharmaceuticals into the environment.

Over the last decade, pharmaceuticals (at trace levels) in the environment and the water cycle (nanograms to low micrograms per liter) have been widely explored. The advancements in analytical techniques and apparatus are primarily responsible for improved detection. Numerous studies have identified many pharmaceuticals in municipal wastewater and effluents as a significant source of drugs in drinking water. Given that raw sewage and wastewater effluents are crucial sources of pharmaceuticals in surface waters, evaluating the efficacy of available control techniques, especially for potable purposes, is imperative.

Biological transformation and chemical adsorption are the most common techniques for removing pharmaceuticals in wastewater treatment plants, employing conventional activated sludge (CAS) systems [57, 58].

Dyes

A dye is a colored, natural, semi-synthetic, or wholly manufactured substance with an affinity for specific substrates while exhibiting distinctive coloration [60]. Dyes are of various structures, often classified based on their chemical

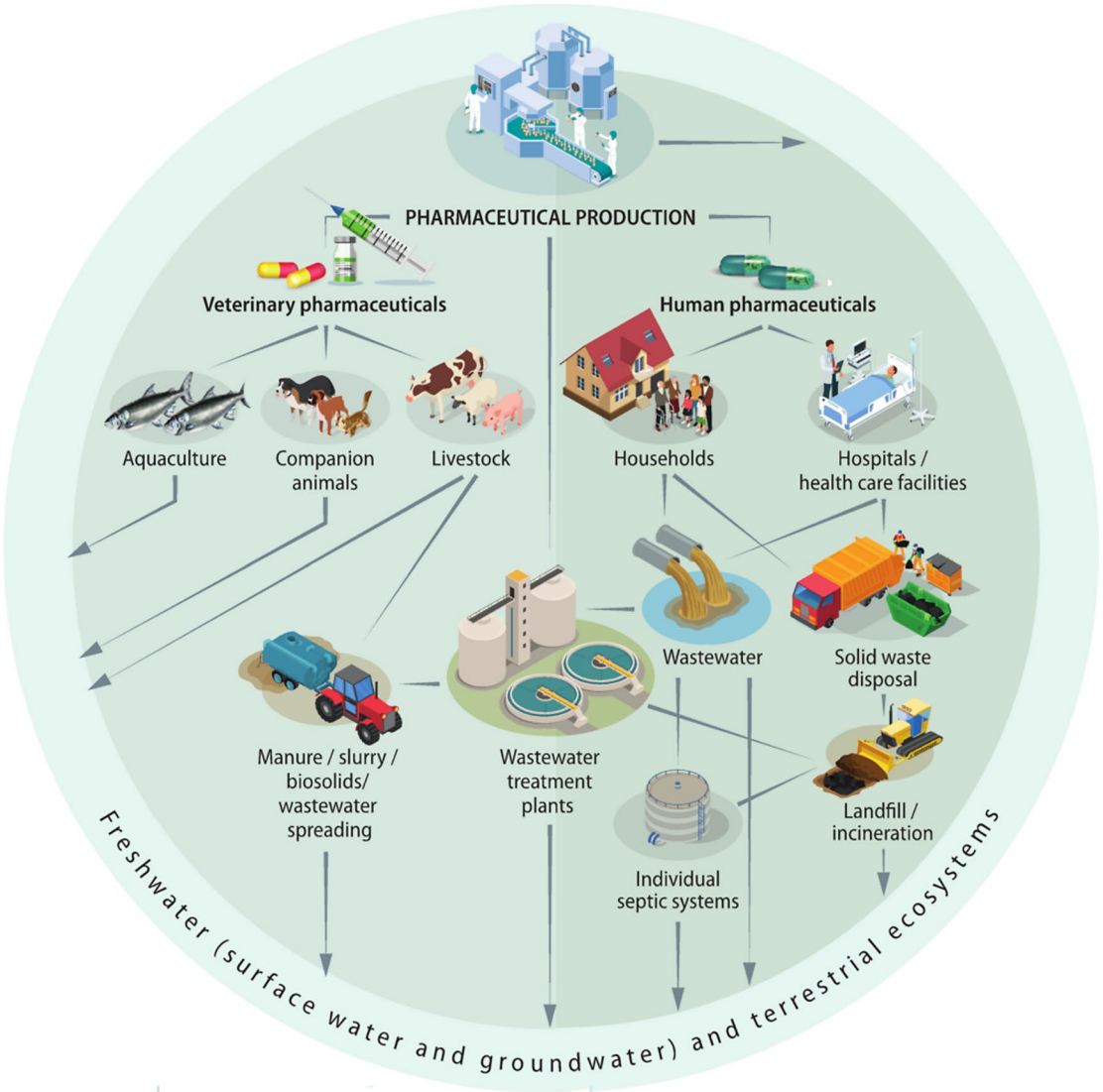

Fig. 1 Major release pathways of pharmaceuticals into the environment [59] (OECD)

contents or application in textile industries. Each dye's color is attributed to the chromophores it bears, linking the auxochromes [61]. Also, dyes can be classified based on the various chromophore groups, with the prominent ones including azo (–N = N–), carbonyl (–C = O), methane (–CH =), nitro ($–NO_2$), and quinoid [62]. The major auxochromes are amine ($–NH_3$), carboxyl (–COOH), sulfonate ($–SO_3H$), and hydroxyl (–OH) [63]. Another chemical reactivity and pH classifications include basic, reactive, dispersion, direct, vat, and azo dyes. All these classes have been explored for wastewater treatment [64]. Table 1 lists common dyes used in textile dyeing procedures.

Reactive dyes are brightly colored organic materials used to tint textile materials. Due to their effective and efficient dyeing qualities, they are widely used in the textile industry. In terms of durability, fiber-reactive dye is the most prominent type. The dye molecule characteristically forms with the cellulose fiber molecule via covalent bonds. Reactive dyes are subdivided into azo, anthraquinone, and phthalocyanin groups [65]. Most common azo dyes are carcinogenic [66]. Their deterioration is similarly hazardous due to their prominent molecular structure.

Amines are formed from the reductive cleavage of azo bonds, making them poisonous and carcinogenic [67]. Azo dyes can change soil's physicochemical properties upon absorption, which annihilates vegetation. If the dyes linger in the soil for an extended period, they may terminate beneficial soil microbes, thereby hindering agricultural output significantly [68, 69]. Due to their excellent coloring qualities, azo dyes dispersed in water are visible to human eye, even in minute concentrations. Dyeing degrades the visual quality of the water and prevents sunlight penetration, altering photosynthesis [70]. This phenomenon depletes the oxygen level and disrupts biological cycles.

Depending on their concentrations, azo dyes are hazardous to the ecology and mutagen. About 109 kg of dyes is generated annually globally, with azo dyes accounting for 70% [71]. Considering large quantities of azo dyes are produced and used frequently in various industries (such as leather tanning, textile, paper, food, etc.), they transform into carcinogenic aromatic amines upon entering the environment. Therefore, improper disposal is a major ecological concern to human and animal health [72]. As a result, it is vital to safeguard the environment from toxic dye effluents and mitigate against human exposure via various physical, chemical, and biological treatments or their combinations. Figure 2 summarizes the impact of textile dyes on several substrates.

Other common organic pollutants

Other organic pollutants of concern include humic substances, phenolic chemicals, petroleum, surfactants, pesticides, polycyclic aromatic hydrocarbons (PAHs), and aromatic amines. For instance, long-term exposure to PAHs can cause cataracts, jaundice, skin redness, inflammation, and kidney and liver damage [83]. Also, inhaling or ingesting concentrated naphthalene can denature red blood cells. Similarly, pesticides can negatively and acutely impact human health (rashes, blindness, nausea, dizziness, diarrhea, and

Table 1 Classification, description, examples, and ecotoxicological effects of dyes

Dye type	Description	Dye example	Ecotoxicological effect	Ref.
Acid	Water-soluble anionic compound	Acid orange 7, acid blue 83, acid blue 7, acid yellow 36	Nausea, vomiting, diarrhea, carcinogenic and mutagenic effects	[74–76]
Basic	Water-soluble, applied in weakly acidic dyebaths, very bright dyes	Basic red 1, basic yellow 2, methylene blue, rhodamine 6G	Alters the physical and chemical properties of water bodies and causes detrimental effects on flora and fauna	[77, 78]
Direct	Water-soluble, anionic compounds, directly applicable to cellulosic without a mordant	Direct red 28, Congo red, direct black 38	Toxic to aquatic animals and plants, carcinogenic, mutagenic, and dermatitis	[79–81]
Disperse	Not water-soluble	Disperse violet 1, disperse red 60, disperse red 9	Carcinogenic and mutagenic; they cause soil and water pollution	[74, 76]
Reactive	Water-soluble, anionic compounds, largest dye class	Reactive red 120, reactive red 147, reactive blue 19	Allergic reaction in eyes, skin, mucous membrane, and the upper respiratory tract	[74, 76]
Sulfur	Organic compounds containing sulfur or sodium sulfide	Sulfur black 1, sulfur blue, sulfur brilliant green, phthalic anhydride	Itchy or blocked nose, skin irritation, carcinogenic, sneezing, and sore eyes	[74, 76]
Vat	Water-insoluble, oldest dyes, more chemically complex	Vat acid blue 74, vat blue 1	Affects the clearness and quality of water resources, dermatitis, rhinitis, allergic conjunctivitis, and other allergic reactions	[75, 77, 82]

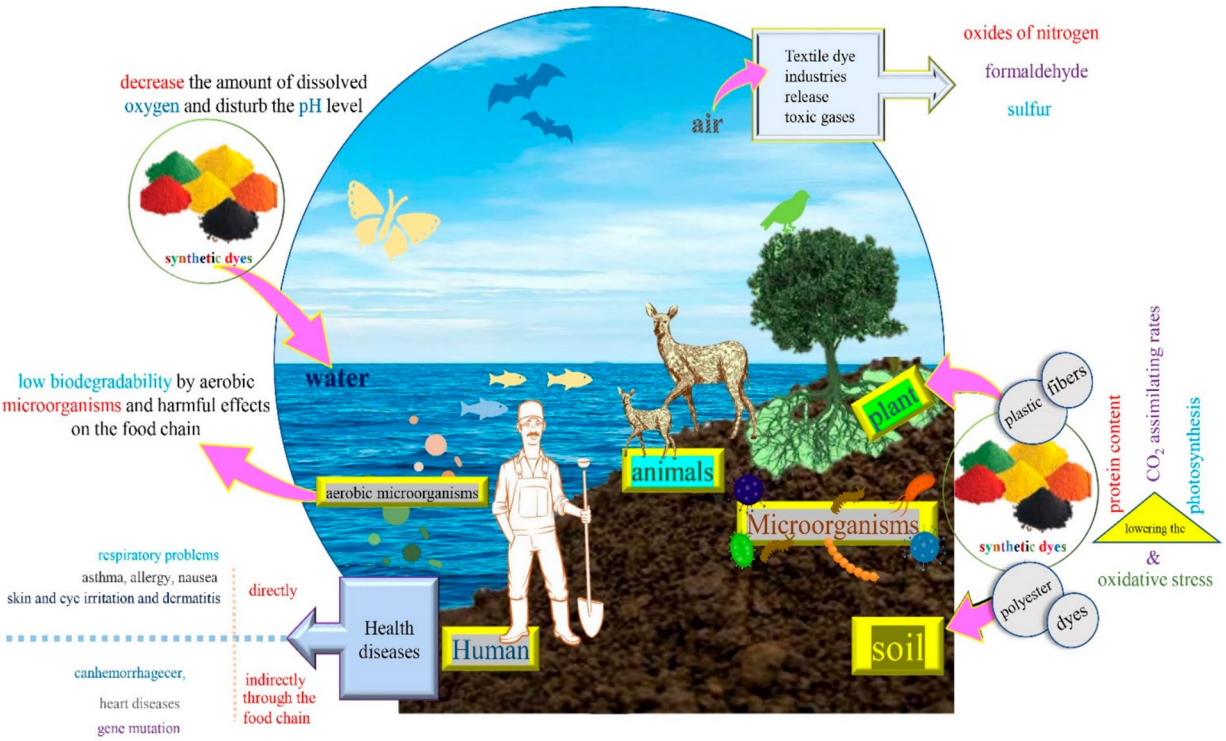

Fig. 2 Effects of textile dyes on several substrates [73]. Reprinted with permission

death), while chronically causing congenital disabilities, reproductive injury, neurological and developmental toxicity, cancer, and endocrine system [84].

Adsorption of pharmaceuticals and dyes

Due to their excellent and distinctive structural properties, graphene-based nanomaterials have been employed to remove various pollutants (including drugs and dyes) from wastewater before environmental disposal [85, 86]. Table 2 summarizes recent reports on the experimental design, target adsorbate, maximum adsorption capacity, etc., of such practices.

For example, using response surface methodology, Yang et al. employed a central composite design to evaluate the operating parameters and identify the ideal conditions for enrofloxacin (ENF) and Rhodamine B (RhB) removal using GO. With an excellent correlation coefficient ($R^2 = 0.9987$ for ENF and $R^2 = 0.9999$ for RhB), the quadratic model effectively characterized the removal efficiency, which increased with the sonication period, pH, and adsorbent amount. pH 7 was the optimum for drug and dye uptake. Elsewhere, Rauf et al. [88] investigated the effect of pH, contact time, temperature, initial MV concentration, and adsorbent dosage in using a magnetic and recyclable montmorillonite/GO/$CoFe_2O_4$ (MMT/GO/$CoFe_2O_4$) nano-composite to clean methyl violet (MV) dye-laden wastewater. The researchers observed that adsorption increased as the pH rose from 2 to 8 before plateauing. The low cationic dye's adsorption at low pH was ascribed to the concentrated H^+ and the ions occupying the active sites on the sorbent. As the initial pH rises, H^+ concentration reduces, and the competition for adsorption sites between H^+ and cationic dye radicals decreases, increasing the adsorption efficiency.

In another investigation, Feng et al. [89] created a new β-cyclodextrin-immobilized reduced GO (β-CD/rGO) to improve naproxen adsorption from aquatic environments. The porous adsorbent had numerous hydroxyl groups and acetalization between the β-CD and the rGO, which enabled a more stable three-dimensional structure. At 313 K, β-CD/rGO exhibited a q_{max} of 361.85 $mg \cdot g^{-1}$ for naproxen. Spent β-CD/rGO could be regenerated with ethanol, making the adsorbent viable for naproxen treatment.

Similarly, Anurag et al. investigated the effect of pH, adsorbent dosage, temperature, and initial drug concentration using rGO-MoS_2 heterostructure to remove ofloxacin antibiotics from an aqueous phase [90]. The 95% maximum removal efficiency at a 0.35 g L^{-1} dosage and 10 mg L^{-1} initial concentration in 4 h was achieved despite the sorbent's low surface area of 17.17 $m^2\ g^{-1}$. The experiment was conducted at pH 4–10, revealing the q_{max} at pH 6 (25 °C). Also, Akpotu and Brenda used MCM-48 encapsulated with reduced GO/GO and as-synthesized MCM-48 to clean up

Table 2 Various experimental designs, conditions, and properties of removing dyes and pharmaceuticals using graphene-based adsorbents

Experimental design	Adsorbate	Adsorbent	Q_{max} ($mg.g^{-1}$)	Adsorption properties	Ref.
Central composite	Enrofloxacin	Graphene oxide (GO)	45.04	Langmuir	[87]
	Rhodamine B		107.2	Freundlich	
–	Methyl violet	Montmorillonite GO/$CoFe_2O_4$	97.26	Langmuir, π–π electrostatic	[88]
–	Naproxen	B-cyclodextrin-reduced graphene oxide	361.8	Langmuir, Pseudo-second order, π–π interactions, Hydrogen bonding, Host–guest interaction	[89]
–	Ofloxacin	Reduced GO-MoS_2	37.31	Langmuir, Pseudo-second order, Exothermic	[90]
–	Caffeine	M48-GO	153.8	Langmuir, Exothermic	[91]
	Phenacetin	M48-graphene	212.7		
Co-precipitation	Sulfamethoxazole	GO-ionic liquid	–	Freundlich, Langmuir, π–π interaction, Hydrogen bonding	[92]
	Reactive blue19				
Hydrothermal	Methylene blue	U10-66$(OH)_2$/GO	–	Freundlich, Pseudo-second order, πvπ interaction, Hydrogen bonding, electrostatic attraction	[93]
–	Methylene blue	Acrylic acid-GO	1448	Langmuir, π–π conjugation, Hydrogen bonding, electrostatic	[94]
	Malachite green		582.1		
	Basic fuchsin		571.7		
	Rhodamine B		437.1		
–	Dopamine	Fe_3O_4-SiO_2/GO/CS/MPTS	215.5	π–π interaction, electrostatic interaction, cation- π interaction	[95]
	Clenbuterol		264.0		
	Orciprenaline		184.2		
	Methylene blue		558.7		
	Crystal violet		613.5		
–	Rhodamine B	$MnFe_2O_4$/graphene	67.8	π–π stacking interaction	[96]
	Crystal violet		81.3		
	Methylene blue		137.7		
	Malachite green		394.5		

pharmaceuticals in aqueous systems [91]. Therein, RGO/GO was successfully encapsulated on MCM-48 after fabrication and characterization of GO/reduced GO MCM-48. The adsorbent's pHpzc significantly impacted the adsorption interface. M48G demonstrated higher adsorption than ASM48 and M48GO, which could be due to its hydrophobic nature. In comparison to basic conditions (pH > pKa), adsorption of CAF and PHE on the adsorbents was highest at acidic pH (pKa). However, because the pH range investigated was below the pKa values of the drugs, the influence of pH on adsorption was minimal.

Ogunleye et al. [92] adopted co-precipitation to adsorb sulfamethoxazole and reactive blue 19 on GO modified with imidazolium-based ionic liquid (Fig. 3). Due to its long chain carbon tail on the adsorbent, the ionic liquid improved the hydrophobicity of the adsorbent, boosting the removal of reactive blue 19 (RB19) dye and sulfamethoxazole (SMZ). Other mechanisms, such as π-π interaction and hydrogen bonding, further aided the adsorption. Sun et al. [93] investigated the parameters influencing MB adsorption onto UiO-66-$(OH)_2$/GO, such as pH, initial concentration, and temperature. The numerous hydroxyl groups on the adsorbent's surface are protonated, making it difficult for the positively charged UiO-66-$(OH)_2$/GO to attach to positively charged MB. As the pH of the solution rises, the H^+ concentration decreases, and the MB cation binds to the adsorption site. The surface groups of the material are deprotonated as the OH level increases, and the adsorbent gradually shifts from positively to negatively charged, exposing more negatively charged adsorption sites. Their results reveal that the UiO-66-$(OH)_2$/GO adsorption kinetics model for MB adsorption follows the pseudo-second-order kinetic model, and the isotherm follows the Freundlich isotherm adsorption model.

Moreover, Wang et al. [94] produced a novel acrylic acid functionalized GO (p(AA)-g-GO) for high-efficiency cationic dye removal and adsorption research (Fig. 4). The study demonstrates a practical approach for synthesizing new p(AA)-g-GO materials by grafting acrylic acid onto the GO surface. The influence of pH on MB adsorption capacity rose from 2 to 10 mg g^{-1}, and the equilibrium adsorption capacity increased from 340.5 to 634.3 mg g^{-1}. The maximum adsorption capacity could be due to high pH stimulation deprotonating -COOH and -OH groups, strengthening the interaction between AGO_2 and MB molecules. Other cationic dyes, malachite green (MG), basic fuchsin (BF), and rhodamine B (RhB), have equilibrium adsorption capabilities of 582.1, 571.7, and 437.1 mg g^{-1}, respectively.

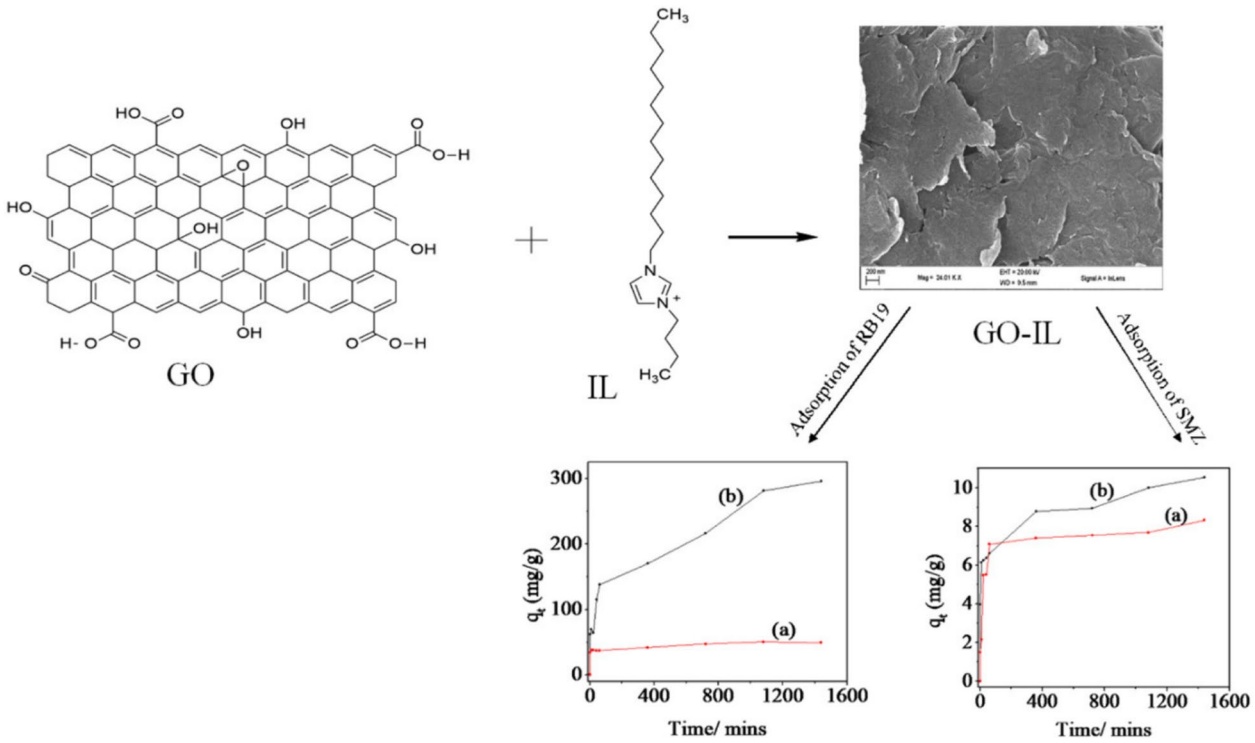

Fig. 3 Synthesis and characterization of sulfamethoxazole and reactive blue 19 on GO modified with imidazolium-based ionic liquid [92]. Reprinted with permission

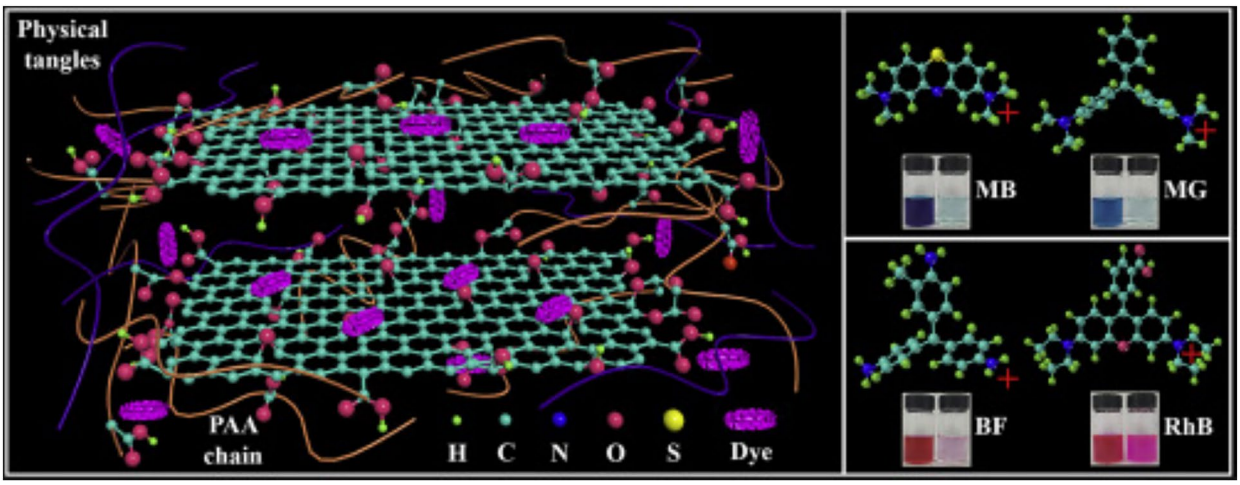

Fig. 4 Performance of acrylic acid functionalized GO (p(AA)-g-GO) for high-efficiency cationic dye removal [94]. Reprinted with permission

In another report, Jiang et al. [95] proposed a simple method for making layer-by-layer GO-based magnetic nano-composites (Fe_3O_4@SiO_2/GO/CS/MPTS) for adsorption removal of β-agonists/dyes and bacterial inactivation in wastewater. At pH 7, the highest elimination efficiency was obtained. Fe_3O_4@SiO_2/GO/CS/MPTS exhibited a zero-point charge of 4.25. The highest adsorption capacity of Fe_3O_4@SiO_2/GO/CS/MPTS for dopamine (DA), clenbuterol (CLE), orciprenaline (ORC), methylene blue (MB), and crystal violet (CV) were 215.52, 263.85, 184.16, 558.66, and 613.50 mg g^{-1}, respectively.

The synthesis and utilization of a graphene-based hybrid nano-composite ($MnFe_2O_4$/G) to mitigate many synthetic dyes, including methylene blue, malachite green, crystal violet, and Rhodamine B, was reported by Thuan et al. [96]. $MnFe_2O_4$/G had a BET surface area of 382.98 m^2 g^{-1}. The

influence of various parameters on the adsorption was investigated, including concentration (5–50 mg L^{-1}), pH (4–10), dosage (5–20 mg), and temperature (25–45 °C). Rhodamine B (67.8 mg g^{-1}), crystal violet (81.3 mg g^{-1}), methylene blue (137.7 mg g^{-1}), and malachite green (394.5 mg g^{-1}) were shown to have the highest adsorption capacity using $MnFe_2O_4$/G.

Adsorption on graphene oxide

Graphene is a novel carbon material made of a single-cell thick planar sheet of sp^2-hybridized carbon with distinct crystal and electrical characteristics [97–99]. The high surface area (2630 m^2 g^{-1} for single-layer graphene) [26, 100], electron transport capabilities [101, 102], high tensile strength [103], and formidable thermal and electrical conductivities [104] have piqued tremendous interest in graphene for research purposes and industry applications. The chemical oxidation of graphite exfoliated in water or organic solvents produces GO, comprising a single layer of graphite oxide [38, 39]. When a strong oxidizing chemical oxidizes graphite, oxygen functionalities (carboxyl, hydroxyl, carbonyl, and epoxy) are tethered into the structure, making it hydrophilic. As a result, graphite oxide is exfoliated in water by sonication, yielding GO, a monolayer or few-layer oxygen-functionalized graphene. On the other hand, graphene oxide (GO) is a graphene type frequently studied as a foundation for graphene synthesis via thermal or chemical reduction methods. Due to the oxygen engraftment, GO may bind with water to form stable suspensions in solutions. The oxidized graphite's hydrophilicity encourages water adsorption into the layered structure, increasing the distance between the layers to 1.15 nm [45].

GO-based nano-composites can be fabricated, adding various functional groups that adapt the material for specific adsorption applications. Courtesy of its surface oxygen-containing functional groups and structural defects, GO has a higher chemical activity than pristine graphene [105]. Because of GO's high chemical reactivity, it can be chemically functionalized, adding additional groups to the GO platelets. Covalent or non-covalent attachments can chemically modify these reactive oxygen functionalities (especially carboxylic, epoxy, and hydroxyl groups). For instance, covalent modification is feasible using polymers to activate, amidate, or esterify carboxyl or hydroxyl groups in GO via coupling processes [106]. Carboxylic acid activation with thionyl chloride [106, 107], 1-ethyl-3-(3-dimethyl aminopropyl)-carbodiimide [108], N, N'-dicyclohexylcarbodiimide (DCC), or coupling octadecylamine with amides [109] are examples of coupling reactions. Moreover, GO epoxy groups can be covalently functionalized via ring-opening reactions, whereby a nucleophilic attack at the α-carbon by the amines takes place [110]. Ring-opening at the epoxy groups can connect an ionic liquid (1-(3-aminopropyl)-3-methylimidazolium bromide; R-NH_2) via its amine end to GO platelets [111].

Besides, GO can be functionalized via silanization. Yang et al. [112] identified covalently bonded 3-aminopropyl triethoxysilane (APTS) on the GO surface by nucleophilic reactions between the GO epoxy and APTS amine groups. Since the silane family provides various terminal functional groups, various solvents (polar or non-polar) can disperse functionalized GO after modification [112, 113]. GO non-covalent functionalization could occur through $\pi-\pi$ stacking, cation $-\pi$ interactions, van der Waals interactions, or hydrogen bonding [114, 115]. For instance, Yang and co-workers [114] adopted non-covalent interactions to prepare a composite containing doxorubicin hydrochloride (DXR) and GO. A strong hydrogen bonding exists between GO's -OH and -COOH groups and the -NH_2 groups of DXR [116]. Due to their high specific surface area and reactivity, GO-based nano-composites are preferred adsorbents for ameliorating organic or inorganic contamination. In addition, the numerous delocalized π-electron systems in GO help generate strong π-stacking interactions with a benzene ring of contaminants.

Factors affecting the adsorption of organic pollutants

Adsorption is influenced by physical and chemical interactions, which depend on the adsorbent's features (surface area, pore size distribution, and surface chemistry), the adsorbate's nature, and the solution's condition (pH, temperature, presence of competitive solutes, ionic strength). Specifically, pore size distribution is particularly decisive in physisorption, determining the accessibility of the sorbate to the pore volume based on the kinetic diameter of the sorptive and the hierarchical pore structure [117]. Physisorption is conditioned in two ways: (i) if the pores are too small, adsorption is hindered; (ii) as the pore size decreases (from macropores to mesopores to micropores), adsorption strength increases and contact points between the adsorbate and the adsorbent increase, inducing adsorption potentials between different pore walls to overlap [118, 119].

On the chemisorption front, the chemistry of the adsorbent surface is solely driven by the availability and amount of the functional groups. It is crucial in adsorption because it affects the carbons' adsorption characteristics and reactivities [120]. The physicochemical features of the adsorbates also influence adsorption because the rate and capacity of adsorption are determined by the type of the adsorbed molecule [121]. The chemical compatibility of the adsorbate and the solution is the focus of the adsorbate-solution interactions. The increase in the hydrophobicity of the adsorbate allows the driving force for adsorbate molecules to escape to

surfaces. The polarity of carbon surfaces influences adsorbent interactions. Hydrophilic surface sites, which may comprise acidic (oxygen-containing) and basic (nitrogen-containing) functionalities, as well as inorganic (metal) species on the adsorbent surface, cause surface polarity. These polar sites serve as the emergent centers of water clusters, obstructing the removal of hydrophobic contaminants by blocking their entrance to the micropores, which contain most of the activated carbon surface area available for adsorption [122]. Creating water clusters is significant for adsorbing contaminants at low concentrations, which is crucial to environmental treatment systems [117].

pH

The pH of a solution affects the surface charge of a contacting adsorbent. The pH also influences site dissociation and the pollutant's solution chemistry. The adsorbents' characteristics, the adsorption mechanism, and the dissociation of adsorbate molecules can all be affected by the pH of the aqueous medium. A solution's pH can also alter the chemical structure of the pollutant by changing the adsorbed ion's surface charge and ionization level [123–128]. Table 3 lists the results of studies examining the effect of initial solution pH. Cationic dyes attach to the adsorbent surface more efficiently in alkaline media, while anionic dyes bind more strongly in acidic media. Typically, HCl and NaOH are used to adjust the pH of aqueous dye/pharmaceutical solutions. Due to electrostatic attraction, introducing HCl protonates the adsorbent's surface, enabling the anionic dye to bind more effectively on its surface. In contrast, adding NaOH deprotonates the adsorbent's surface, creating a repulsive interaction between the anionic dye and the sorbent.

Temperature

Temperature is also a major physicochemical factor that affects adsorption mechanisms by changing the reaction from endothermic to exothermic or vice versa [139]. Temperature affects adsorption, plausibly shifting adsorption quantity [140]. Temperature can also influence sorption efficiency depending on the adsorbent and the pollutant. In general, it improves the adsorption of contaminants by raising the adsorbate's surface activity and kinetic energy. If chemisorption ensues, it is favored by higher temperatures because the rate of chemical reaction increases with temperature. Conversely, if the sorption process is physisorption, the higher temperature will hinder the adsorption because most physisorptions are exothermic. The adsorbent's adsorption sites and activity can change chemically due to temperature change [141].

Endothermic and exothermic processes are distinguishable. In an exothermic reaction, the efficacy of the adsorption process reduces as temperature rises. This occurrence can be explained by the fact that when the temperature increases, the intermolecular interactions at the adsorption interface weaken [142]. Because the mobility of the pollutant ions increases when heat is applied to the solution, exothermic adsorption is typically utilized to regulate the intraparticle diffusion [143]. On the other hand, as the temperature rises, the efficiency improves because more active sites are available due to the sorbent surface's activation at higher temperatures [144]. Overall, enhanced adsorption at higher temperatures may indicate an endothermic process rather than exothermic, especially at lower temperatures.

Table 4 illustrates the results of studies investigating the effect of temperature.

Table 3 Results of various research on the effect of initial solution pH on the removal of dye/pharmaceuticals using GO-based adsorbent

Dye/Pharmaceutical	Adsorbent	Ionic Nature	pH	Increase of pH (↑)	Ref.
Methylene blue	β-cyclodextrin/poly(acrylic acid)/GO	Cationic	2–12	mg g^{-1} ↑	[129]
Safranine	β-cyclodextrin/poly(acrylic acid)/GO	Cationic	2–12	mg g^{-1} ↑	[129]
Ethyl violet	Xylan/poly(acrylic acid)/GO	Cationic	2–9	E% ↑	[130]
Malachite green	Zeolitic imidazole GO	Cationic	3–6	E% ↑	[131]
Basic red 46	GO	Cationic	1–6	E% ↑	[132]
Methylene blue	Zeolite-A/reduced GO	Cationic	2–11	q(mg.g^{-1}) ↑ 335.2 to 394.6	[133]
Sulfamethoxazole	Silica-magnetic GO	–	5–9	q(mg.g^{-1}) ↓	[134]
Naproxen	Silica-magnetic GO (GO-MNPs-SiO_2)	–	2–10	E% ↓	[135]
Phenazopyridine	Magnetite-GO	–	3–8	E% ↑	[136]
Dorzolamide	GO-poly(acrylic acid)	–	3–9	E% ↓	[137]
Chlorpheniramine	GO-iron oxide	–	2–11	q(mg/g) 77 to 318 ↑	[138]

*E% is the efficiency of the adsorption process

Table 4 Results of studies on the effect of temperature on the removal of dye/pharmaceuticals using GO-based adsorbent

Dye/Pharmaceutical	Adsorbent	Temperature (K)	Type of Process	q_e(mg.g^{-1})	Ref.
Malachite green	Starch-graft poly (acrylamide) GO/ hydroxyapatite	298–328	Endothermic	297	[145]
Methylene blue	GO-Zeolite	298–318	Endothermic	82.15–97.35	[146]
Acid orange 8	GO	293	–	29	[147]
Direct red 23	GO	293	–	15.3	[147]
Rhodamine	Reduced-GO-nickel	–	Endothermic	47.62	[148]
Methylene blue	Magnetic GO	–	Endothermic	32.56–1430	[149]
Amoxicillin	Magnetic graphene nanoplatelets	293–313	Exothermic	14.10	[150]
Aminophen	GO composites	–	–	13.7	[151]
Carbamazepine	GO composites	–	–	11.2	[151]
Tetracycline	Graphene	293	Endothermic	272.7	[152]
	KOH-activated graphene			532.6	
Ciprofloxacin	Magnetic Polyaniline/GO	298–318	Endothermic	106.38	[153]
Chlorotetracycline	Magnetic GO	313	Endothermic	162.4	[154]
Tetracycline hydrochloride				106.6	
Oxytetracycline				145.9	
Chlorotetracycline	GO/TiO_2	298	Endothermic	261.1	[155]

Concentration

The initial concentration of pollutants is also one of the most vital factors influencing adsorption. It indirectly impacts the effectiveness of dye/pharmaceutical removal by altering the binding site availability on the sorbent. The efficiency of pollutant removal and the maximum amount of the pollutants bound in equilibrium are directly correlated to the concentration of the initial pollutant [156, 157], as expressed in Eqs. 1 and 2.

$$E(\%) = \frac{C_i - C_f}{C_f} \times 100 \quad (1)$$

$$q = \frac{(C_i - C_f) \times V}{m} \quad (2)$$

where E (%) is efficiency, q (mg·g^{-1}) is the amount of pollutants bound in equilibrium, C_i (mg·L^{-1}) is initial concentration, C_f (mg·L^{-1}) is the final concentration, m (g) is the amount of adsorbent, and V is the volume of the aqueous solution. Three tendencies may be seen when looking at the influence of initial pollutant concentration: (a) removal efficiency declines as initial concentration increases; (b) removal efficiency increases as initial concentration increases; (c) no appreciable change in removal efficiency. Table 5 lists the results of studies investigating the effect of initial concentration on the efficiency of GO-based adsorbents in removing dyes and drugs from polluted water samples.

Specific surface area

An essential component of sorption processes is specific surface area (SSA), the total surface area of a solid material divided by its mass. SSA is influenced by particle size, the material's structure, and porosity [162]. Two factors determine how adsorption capacity and particle size relate to one

Table 5 Results of studies on the effect of initial concentration on removing dye/pharmaceuticals using GO-based adsorbent

Dye/Pharmaceutical	Adsorbent	Concentration (mg. L^{-1})	Reaction time (min)	Efficiency (%)	Refs.
Acid orange 7	Cobalt ferrite-reduced GO	5–30	120	92.11–79.45	[158]
Methylene blue	Polyaniline-GO@$SrTiO_3$	10–50	–	99.0–89.6	[159]
Methyl orange	Polyaniline-GO@$SrTiO_3$	10–50	–	95.01–81.75	[159]
Malachite green	Poly(methylmethacrylate/GO-Fe_3O_4	1–7	35	Increased	[160]
Malachite green	Poly(methylmethacrylate/GO)	1–7	35	Increased	[160]
Tetracycline	MnO_2/graphene	100–1000	–	–	[161]

Table 6 Results of studies on the effect of specific surface area on the removal of dye/pharmaceuticals using GO-based adsorbent

Dye/Pharmaceutical	Adsorbent	Specific surface area ($m^2.g^{-1}$)	q_e ($mg.g^{-1}$)	Ref.
Crystal violet	Reduced-GO Zeolitic imidazolate-67	491	1714	[164]
Methyl orange	Reduced-GO Zeolitic imidazolate-67	491	426.3	[164]
Crystal violet	Gum tragacanth/GO	283.84	94	[165]
Congo red	Gum tragacanth/GO	283.84	101.7	[165]
Congo red	NiO/graphene	26.10	123.9	[166]
Tetracycline	Nitrilotriacetic acid-magnetic GO	24	109	[167]
Tetracycline	Diethylenetriaminepentaacetic acid functionalized magnetic GO	176	–	[168]
Ciprofloxacin	Porous graphene hydrogel	231.38	235.6	[169]
Fluoroquinolone	Polydopamine@GO/Fe_3O_4	50.34	70.9	[170]
Ciprofloxacin	Magnetic chitosan-GO	388.3	282.9	[171]
Sulfamethazine	Graphene	271.10	104.9	[172]

another: (a) the chemical structure of the dye molecule and its capacity to produce hydrolyzed species determine the link between adsorption capacity and particle size, and (b) the adsorbent's properties. Since there are more active sites for binding, smaller particle sizes increase adsorption capacity and efficiency in batch techniques [163]. Table 6 provides research findings on the effect of SSA on such adsorptions. Small particle size may lower the adsorption capacity depending on the type of adsorbent.

Adsorption capacity and selectivity

Surface functionalization of nanomaterials is a simple technique that improves selectivity and specificity against contaminants [173]. Dissolved organics in water can severely diminish adsorbents' performance and capacity. Factors that contribute to lowering adsorbent efficiency toward dissolved organics include the following: (i) dissolved organic materials are often concentrated than other aqueous pollutants; (ii) dissolved organic materials may strive with pollutants through various mechanisms, such as competition for adsorption sites and pore blockage; and (iii) dissolved organic materials do not readily desorb due to its high molecular weight and ability to bind at multiple sites [174]. Though achieving several goals in a single treatment procedure may be challenging, understanding the interactions between dissolved organic materials and adsorbent is critical for optimizing their removal from water, minimizing their impact on the removal of target pollutants, or both. The two fundamental interactions that control the extent of dissolved organic materials adsorption by adsorbent are size exclusion and adsorption processes [175]. Two primary factors determine an adsorbent's capacity for dissolved organic materials: (i) carbon surface acidity vs. dissolved organics' composition and (ii) carbon pore size vs. molecular size. As the surface and adsorbate macromolecules are chemically compatible, adsorbent capacity should rise as the size of dissolved organic materials decreases. Repulsive forces may significantly reduce adsorption capacity between strongly acidic functionalities (such as carboxylic groups) on the adsorbent surface and within the dissolved organic materials structure [176].

Sorbate-sorbent interface

The adsorption mechanism is essential to developing an adsorption application. Usually, the total area per unit volume determines the adsorption capacity. The active sites on the exterior surface are more open to adsorbates than those on the inner pore walls, both contributing to the total adsorption capacity [177]. Although graphene has a large surface area, the material is not permeable. As a result, introducing pores improves its adsorption capacity. Another technique to increase graphene's adsorption capacity is introducing various functional groups onto the surface, which show significant affinity toward the adsorbates of interest. The functional groups help the adsorbent and adsorbate to form bonds.

Oxidizing graphene makes it hydrophilic by functionalizing its surface with groups like –CO, –COOH, and –OH. Thus, graphene-based materials attract organic dyes and pharmaceuticals via hydrogen bonding, electrostatic, or π–π conjugation interactions at the interface [178, 179].

Graphene oxide is an efficient dye adsorbent due to its unique conjugated, two-dimensional structure. GO sheets have several oxygen-rich functional groups that create negative charges. GO sheets are highly dispersed in water, inhibiting the separation of dye-adsorbed GO sheets from the aqueous phase. As a result, numerous modified GO-based nanomaterials have been produced to facilitate dye and pharmaceutical separation from aqueous environments. For example, Uio-66-$(OH)_2$/GO was developed by Sun

et al. [93] for the adsorptive removal of dye and antibiotics from water. Methylene blue (MB) adsorption on UiO-66-$(OH)_2$/GO combines physisorption and chemisorption. The strong chemical bonding force between the metal and the MB molecule may be responsible for MB adsorption on UiO-66-$(OH)_2$/GO, considerably improving the adsorption efficiency.

Furthermore, under different acid–base environments, the material's surface electronegativity varies somewhat, affecting the electrostatic interaction between the adsorbent and the adsorbed substance. Tetracycline hydrochloride (TC) adsorption by UiO-66-$(OH)_2$/GO is also influenced by the π-π interaction and hydrogen bonding. Hydrogen bonding and the π-π interaction are crucial in the interaction between GO and TC. The amine group in the TC molecule is basic, whereas the Zr-O cluster in UiO-66-$(OH)_2$/GO has partial Lewis acid characteristics, and the acid–base interaction is another chemisorption mechanism. According to Zheng et al. [180], electrostatic attraction and ion exchange processes are responsible for the adsorption of anionic dyes like CR and MO on GO–NiFe–LDH. The ion exchange method also involves the exchange of ions between the adsorbate and the adsorbent.

Elsewhere, Matej et al. [181] used molecular modeling to create the most comprehensive adsorption dataset for pristine and functionalized graphene interacting with antibiotics, such as 8-lactams, 3 macrolide, 12 quinolone, 4 tetracycline, 15 sulphonamide, trimethoprim, 2 lincosamide, 2 phenicole, and 4 nitroimidazole, and their transformation products in water and *n*-octanol. The results demonstrate that adsorption is aided by combining non-covalent interactions, such as van der Waals dispersion forces, π-interactions, hydrophobic interactions, and hydrogen bonding. Regarding chemisorption, Ahmed et al. [182] describe the mechanism of gemfibrozil (GEM) adsorption by the graphene-based composite foam. The high correlation coefficients show that the adsorption equilibrium of GEM by the foam material followed the Langmuir isotherm model. The Langmuir isotherm is a good model for illustrating a chemical adsorption process in which the adsorbent and adsorbate generate chemical interactions between their reactive groups that are either ionic or covalent.

Similarly, Liu et al. [183] described the adsorption mechanism of graphene-based hyper-cross-linked porous carbon (GN/HCPC) composite to consist of pore filling, hydrogen bonding, and π-π interactions between the adsorption material and the pollutant molecules (Fig. 5). Prarat et al. [184] proposed that oxytetracycline antibiotic (OTC) adsorption onto amino-functionalized mesoporous silica-magnetic graphene oxide nano-composites (A-mGO-Si) was driven by H-bonding and π–π EDA interactions. Also, the cation–π interactions between π electron of GO and $–NH_2^+$ of OTC are other possible mechanisms. Li et al. [185] stressed that H-bonding between OH and COOH groups, π-π interaction, cation-π bonding between protonated amino groups in tetracycline (TC) molecule, π-electron-rich structures of the nitrilotriacetic acid-functionalized magnetic graphene oxide (NDMGO), and amidation reactions are the leading mechanism for TC adsorption.

In summary, the various adsorption mechanism processes are illustrated in Fig. 6

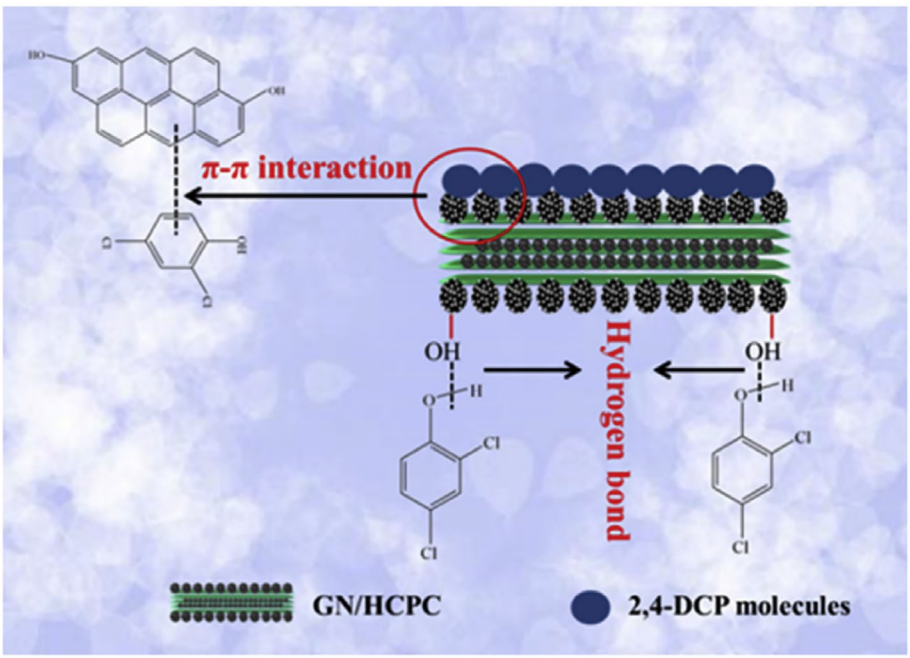

Fig. 5 Adsorption mechanism of 2,4-DCP on the GN/HCPC composite [186]. Reprinted with permission

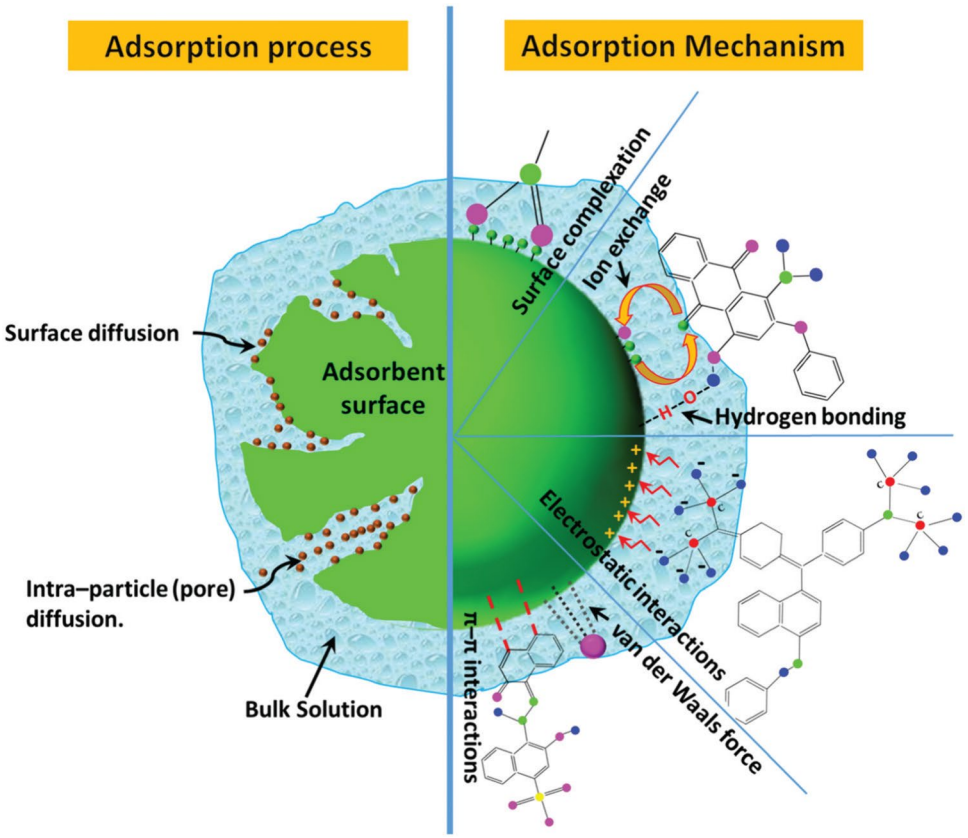

Fig. 6 Adsorption mechanism processes [187]. Reprinted with permission

Adsorption properties

The adsorption rate is often determined via the kinetic studies. Adsorption kinetics models provide information on the adsorption equilibration time and maximum adsorption rate [188]. Usually, the experimental results are fitted into various kinetics models. Pseudo-first-order kinetic, pseudo-second-order kinetic, intraparticle diffusion, and Elovich models are popular adsorption kinetics models. In theory, the adsorption rate can be determined by several processes: (i) transfer of the adsorbate from the bulk solution to the solid phase's surface; (ii) adsorbate passage through the liquid film attached to the solid surface (film diffusion); (iii) internal mobility via pore dispersion from the solid phase's surface to the inner surface of the porous structure (intra-particle diffusion); (iv) solute diffusion on the adsorption sites of the solid phase bringing about physisorption and chemisorption on the solid phase surface. The variability in the reaction steps, with varied speeds, determines the degree of adsorbate removal. When adsorption occurs, there is a temperature difference between the adsorbent and the bulk fluid [189]. The rate of heat and mass transfer determines the temperature variation.

Using the pseudo-second-order model, Kong et al. [190] investigated the kinetics of cadmium (Cd^{2+}), safranin-O (SO), crystal violet (CV), and methylene blue (MB) adsorption on nitrogen and sulfur co-doped graphene-based aerogel (GBA) modified with 2,5-dithiobisurea. The pseudo-second-order kinetic model had the highest correlation coefficient ($R^2 > 0.96$). Theoretical adsorption capacity values for Cd^{2+}, SO, CV, and MB computed using the pseudo-second-order model were 1.354, 0.825, 0.459, and 0.314 mmol g^{-1}, respectively, agreeing excellently with the experiment value. These findings confirm the sharing or exchange of electrons at the interface as the primary adsorption mechanism. In another study, Lagergren's first-order and pseudo-second-order models investigated the kinetics of crystal violet adsorption on the Fe_3O_4/porous graphene nano-composite. Here, the pseudo-second-order kinetic model was the most suitable for the adsorption [191].

Likewise, thermodynamic parameters can be utilized as indexes to determine adsorption feasibility. They inform on the equilibrium between the adsorbent and the aqueous phase, i.e., equilibrium is reached when a system is in its lowest Gibbs energy state. Thermodynamic properties are usually used for expressing adsorption systems in two ways: (i) directly assessable properties comprising temperature and equilibrium constant, and (ii) properties that cannot be measured directly, such as Gibbs energy change, enthalpy change, entropy change, activation energy, and isosteric heat of adsorption [192]. The study of such thermodynamic

characteristics elucidates the mechanism and performance of adsorption.

Anna and Constantine [193] described the feasibility and spontaneity of the process of estriol adsorption on reduced graphene oxide, GO, and their magnetite composites (MGr and MGO). The parameters were calculated and assessed at 25, 35, and 45 °C, as well as the optimum pH for the samples. The $\Delta G°$ values for the samples were negative at all temperatures, indicating that adsorption happens spontaneously. Furthermore, as the temperature was raised, $\Delta G°$ rose, showing that low temperatures favor estriol adsorption. The adsorption was inferred to be primarily physical based on the computed $\Delta G°$ values (> 20 kJ mol). The sorption evinced negative $\Delta H°$ values, indicating an exothermic process in which the total energy required for bond formation between adsorbate and adsorbent was higher than the total energy absorbed in bond breaking. Low $\Delta S°$ values indicate reduced randomness during adsorption at the solid/solution interface. The negative values of ΔG, ΔH, and ΔS indicate that estriol uptake is governe^{-1}d by enthalpy.

Adsorbent reusability

Adsorbent regeneration is vital to real-life applications because it demonstrates the adsorbent's reusability and reliability. Regeneration is the process by which sorbate-laden adsorbent is refreshed by desorbing the sorbate molecules. Desorptions are usually accomplished through ion exchange or pH change. New desorption approaches, such as heat treatment [187, 194, 195], bio-regeneration [196], microwave irradiation [197], and ultrasonic regeneration [198], have recently gained a lot of attention. Desorption is also frequently accomplished through chemical extraction utilizing desorption agents such as NaOH, HCl, H_2SO_4, EDTA, NH_4Cl, NH_4NO_3, acetic acid, and phosphoric acid, among others. Temperature and concentration are two elements that affect desorption. Table 7 lists the results of various studies involving the regeneration of dye- or pharmaceutical-laden adsorbents.

Comparison of graphene-based nanomaterials with other adsorbents

Generally, adsorbents are porous solid substances with high surface thermal stability, durability, and adsorption capacity over various adsorbate concentrations. These materials have unique pore dimensions that allow speedy mobilization of gaseous vapors or substances in solution and a short intraparticle distance [210, 211]. Moreover, an adsorbent should be earth-abundant and cost-effective. Various adsorbents have been successfully utilized in decontaminating wastewater laden with toxic pollutants. For example, zeolites are excellent adsorbents because of their unique ion exchange capability to eliminate undesirable cations [212]. Zeolites

Table 7 Results of studies involving regeneration and re-use of dye- or pharmaceutical-laden adsorbents

Sorbate	Sorbent	q_{max} (mg g^{-1})	Removal efficiency (%)	No of cycles	Ref.
Ranitidine, Carbamazepine, and Chlorothiazide	Crosslinked chitosan/nitrogen doped-graphene quantum dot nano-composites	–	> 50	5	[199]
Azo blue, Methylene blue, Orange G, and Fluoride	Crosslinked chitosan/nitrogen doped-graphene quantum dot nano-composites	–	74, 73, 84, and 34	5	[199]
Metformin	Graphene oxide	50.47–31.60		5	[200]
PHE and CAF	M48G, M48GO	–	83 and 76, 45 and 30	4	[91]
Methyl blue and methyl orange	Graphene oxide-manganese oxide	–	90	7	[201]
Methyl orange	MCA, G/MCA, MCA-C, and G/MCA-C	–	82, 86, 96, and 99 to 80, 84, 88, and 90	3	[202]
Rhodamine B	Reduced graphene oxide-nickel (RGO–Ni)	–	85	6	[203]
Methylene blue and methyl violet	$CoFe_2O_4$ loaded graphene oxide	48.2–10.6 8.7	–	4	[204]
Rhodamine B	Bi_2O_3@GO nanocomposite	320	78%	8	[205]
Methylene blue and Rhodamine	Graphene oxide hydrogel	122.5	100–95 95–85	3	[206]
Basic blue 26	Carbon nitride /GO	917.78	89–74	5	[207]
Norfloxacin	N-RGO/Fe_3O_4	126.5- 73.3	81.7–63.5	3	[208]
Ciprofloxacin	MGO@PANI	–	96.7–47	15	[209]

Table 8 Comparison of the advantages and disadvantages of various nanomaterials

Materials	Advantages	Disadvantages
Carbon nanotubes	High adsorption capacity, large surface area, reusable, ease of modification	Toxicity, high cost of production
Activated carbons	Carbon-based material with highly developed pores and surface area	Reusability and regeneration costs are high, drastically reducing its application
Chitosan-based sorbents	Eco-friendly, readily available and reusable, simple to prepare and modify, non-toxic and selective	Crosslinker is needed and less stable for a long time
Metal oxide-based sorbents	Selective and specialized towards a specific contaminant due to its charged nature. Large surface area and good adsorption capacity	Agglomerate, due to attractive forces, is toxic and harmful to one's health; separation is difficult, has poor mechanical strength, and is less stable
Graphene-based sorbents	The capacity of graphene to remove various pollutants, large surface area, and good capability to be functionalized, chemical functionalization helps to prevent agglomeration and improves sensitivity and selectivity	Simultaneous separation of graphene and graphene oxide is slow

exist in nature as aluminosilicate crystals. They consist of numerous assorted minerals, including clinoptilolite, which is highly abundant in nature and is found in more than 40 naturally occurring zeolites [213].

On the other hand, peat moss is ubiquitous and readily obtainable across the U.S. and Europe. It exhibits high surface area and porosity, enabling its selective affinity toward toxic cations [214]. Similarly, activated carbons (including coal-derived sorbents) are non-crystalline carbon-based materials with highly developed pores and surface areas [215–217]. However, its reusability and regeneration costs are high, drastically reducing its application as an adsorbent.

In the quest for improved carbon materials for adsorption, newer carbon-based nanomaterials (such as carbon nanotubes, carbon nanofibers, fullerenes, the graphene family, etc.) have been investigated. Because of its impressive electrical, mechanical, and chemical capabilities and affordable production costs compared to other adsorbents, graphene-based nanomaterials have been employed for diverse adsorption of organic pollutants such as dyes, pharmaceuticals, and other organic contaminants. Graphene-based nano-composites are being studied as interesting adsorbent materials owing to their outstanding properties [217]. The capacity of graphene to remove various pollutants and its dispersion in the liquid phase are both essential factors in its application as nano adsorbents. Graphene can agglomerate and restack to yield graphite during wastewater treatment. Simultaneous separation of GO and graphene is tedious. During treatment, chemical functionalization helps to prevent agglomeration. It also improves their interaction with various organic and inorganic contaminants. Adding nanoparticles or other functional components to the graphene surface improves their sensitivity and selectivity. Layered graphene shows a high surface area and good functionalization capability by different covalent and non-covalent modifications [218, 219]. In summary, the merits and demerits of these adsorbents are compared in Table 8.

Conclusion and prospects

In summary, graphene-based nano-composites are of interest to fundamental research and industrial use. An overview of the adsorbents shows their capacities for adsorbing pharmaceuticals and dyes. More attention should be focused on the current shortcomings, such as graphene oxide synthesis, functionalization, structure, and analysis/characterization methods. But despite all these shortcomings, graphene-based materials still show advantages in fundamental research and industrial uses. Studies on graphene-based nano-composites are increasing rapidly due to their enormous and unique properties. Researchers have been competing to develop novel nano-composites, adopting various synthesis methods. The synthesis method is crucial to large-scale production and controlling the nano-composite's quality. At the same time, the procedures should be efficient, affordable, and environmentally benign. Therefore, future research should deploy two-dimensional GO sheets for advanced technological applications in remediating dye and pharmaceutical-laden wastewaters.

Acknowledgements The authors acknowledge the assistance of their research colleagues at the Department of Marine Science and Technology of The Federal University of Technology, Akure, Nigeria.

Funding This research was not funded by any person or organization.

Availability of data and materials Authors will make the data available upon request to the Corresponding author.

Declarations

Conflict of interest The authors declare no conflicts of interest.

Compliance with ethical standards Not applicable.

Consent to participate This article does not involve any human subjects.

References

1. Ming HW (2013) Environmental contamination health risks and ecological restoration, Taylor and Francis group. Earth Sci Eng Technol 518
2. Rizwana Q, Muneeb AF (2019) Freshwater pollution: effects on aquatic life and human health. Fresh Water Pollut Dyn Rem, pp 15–26
3. World Health Organization (2022) Drinking water
4. Fella H-C, Mohamed BE (2019) Water quality and physico-chemical parameters of outgoing waters in a pharmaceutical plan. Appl Water Sci 9:165
5. Sharma VK, Feng M (2019) Water depollution using metal-organic frameworks-catalyzed advanced oxidation processes: a review. J Hazard Mater 372:3–16
6. Kumar A, Khan M, He J, Lo I (2020) Recent developments and challenges in practical application of visible–light–driven TiO_2–based heterojunctions for PPCP degradation: a critical review. Water Res 170:115356
7. Rosman N, Salleh W, Azuwa M, Jaafar J, Ismail A (2018) Hybrid membrane filtration-advanced oxidation processes for removal of pharmaceutical residue. J Colloid Interf Sci 532:236–260
8. Sane PK, Tambat S, Sontakke S, Nemade P (2018) Visible light removal of reactive dyes using CeO_2 synthesized by precipitation. J Environ Chem Eng 6:4476–4489
9. Saitoh T, Shibata K, Hiraide M (2014) Rapid removal and photodegradation of tetracycline in water by surfactant-assisted coagulation–sedimentation method. J Environ Chem Eng 2:1852–1858
10. Sheng C, Nnanna A, Liu Y, Vargo JD (2016) Removal of Trace Pharmaceuticals from Water using coagulation and powdered activated carbon as pretreatment to ultrafiltration membrane system. Sci Total Environ 550:1075–1083
11. Al-Rifai JH, Khabbaz H, Schafer A (2011) Removal of pharmaceuticals and endocrine disrupting compounds in a water recycling process using reverse osmosis systems. Sep Purif Technol 77:60–67
12. Yadav A, Sharma P, Baran A, Kumar V (2021) Photocatalytic TiO_2 incorporated PVDF-co-HFP UV-cleaning mixed matrix membranes for effective removal of dyes from synthetic wastewater system via membrane distillation. J Environ Chem Eng 9:105904
13. Luiza D, Demarchi C, Danielle F, Melo C, Rodrigues C (2016) Adsorption of rhodamine B and methylene blue dyes using waste of seeds of *Aleurites Moluccana*, a low cost adsorbent. Alexandria Eng J 55:1713–1723
14. Khan S, Naushad M, Al-Gheethi A, Iqbal J (2021) Engineered nanoparticles for removal of pollutants from wastewater: current status and future prospects of nanotechnology for remediation strategies. J Environ Chem Eng 9:106160
15. Ali M, Hoque M, Safdar H, Biswas M (2020) Nanoadsorbents for wastewater treatment: next generation biotechnological solution. Int J Environ Sci Technol 17:4095–4132
16. Priya A, Gnanasekaran L, Rajendran S, Qin J, Vasseghian Y (2022) Occurrences and removal of pharmaceutical and personal care products from aquatic systems using advanced treatment—a review. Environ Res 204:112298
17. Singh S, Kumar V, Anil AG, Kapoor D, Khasnabis S, Shekar S, Pavithra N, Samuel J, Subramanian S, Singh J, Ramamurthy PC (2021) Adsorption and detoxification of pharmaceutical compounds from wastewater using nanomaterials: a review on mechanism, kinetics, valorization and circular economy. J Environ ManagE 300:113569
18. Hamad HN, Idrus S (2022) Recent developments in the application of bio-waste-derived adsorbents for the removal of methylene blue from wastewater: a review. Polymers 14:783
19. Ponnuchamy M, Kapoor A, Kumar PS, Vo D-VN, Balakrishnan A, Jacob MM, Sivaraman P (2021) Sustainable adsorbents for the removal of pesticides from water: a review. Environ Chem Lett 19:2425–2463
20. Slater A, Cooper A (2015) Function-led design of new porous materials. Science 348:988–1008
21. Ariga K, Li J, Fei J, Ji Q, Hill JP (2016) Nanoarchitectonics for dynamic functional materials from atomic-/molecular-level manipulation to macroscopic action. Adv Mater 28:1251–1286
22. Benzigar M, Talapaneni S, Joseph S, Ramadass K, Singh G, Scaranto J, Ravon U, AlBahily K, Vinu A (2018) Recent advances in functionalized micro and mesoporous carbon materials: synthesis and applications. Chem Soc Rev 47:2680–2721
23. Lakhi K, Park D, AlBahily K, Cha W, Viswanathan B, Choy J, Vinu A (2017) Mesoporous carbon nitrides: synthesis, functionalization, and applications. Chem Soc Rev 46:72–101
24. Shahin H, Mady E (2017) Graphene membranes for water desalination. NPG Asia Mater 9:e427
25. Rasel D, Eaqub A, Sharifah BAH, Seeram R, Zaira ZC (2014) Carbon nanotube membranes for water purification: a bright future in water desalination. Desalination 336:97e109
26. Stoller MD, Park S, Zhu Y, An J, Ruoff RS (2008) Graphene-based ultracapacitors. Nano Lett 8:3498–3502
27. Balandin AA, Ghosh S, Bao W, Caliza I, Teweldebrhan D, Miao F, Lau CN (2008) Superior thermal conductivity of single-layer graphene. Nano Lett 8:902–907
28. Novoselov KS, Geim AK, Morozov SV, Jiang D, Zhang Y, Dubonos SV, Grigorieva IV, Firsov AA (2004) Electric field effect in atomically thin carbon films. Science 306:666–669
29. Lee C, Wei X, Kysar JW, Home J (2008) Measurement of the elastic properties and intrinsic strength of monolayer graphene. Science 321:385–388
30. He HK, Gao C (2011) Graphene nanosheets decorated with Pd, Pt, Au, and Ag nanoparticles: Synthesis, characterization, and catalysis applications. Sci China Chem 54:397–404
31. Liu GL, Yu CL, Chen CC, Ma WH, Ji HW, Zhao JC (2012) A new type of covalent-functional graphene donor-acceptor hybrid and its improved photoelectrochemical performance. Sci China Chem 55:1622–1626
32. Abdelhamid HN, Wu HF (2013) Multifunctional graphene magnetic nanosheet decorated with chitosan for highly sensitive detection of pathogenic bacteria. J Mater Chem B 1(32):3950–3961
33. Chen S, Zhu J, Wu X, Han Q, Wang X (2010) Graphene oxide-MnO_2 nano-composites for supercapacitors. ACS Nano 4 (5): 2822e2830
34. Khan MS, Abdelhamid HN, Wu H-F (2015) Near infrared (NIR) laser mediated surface activation of graphene oxide nanoflakes for efficient antibacterial, antifungal and wound healing treatment. Colloids Surf B 127:281–291
35. Rizzo L, Fiorentino A, Grassi M, Attanasio D, Guida M (2015) Advanced treatment of urban wastewater by sand filtration and graphene adsorption for wastewater reuse: Effect on a mixture of pharmaceuticals and toxicity. J Environ Chem Eng 3(1): 122e128
36. Manikandan M, Abdelhamid HN, Talib A, Wu H-F (2014) Facile synthesis of gold nanohexagons on graphene templates in Raman spectroscopy for biosensing cancer and cancer stem cells. Biosens Bioelectron 55:180–186

37. Shao G, Lu Y, Wu F, Yang C, Zeng F, Wu Q (2012) Graphene oxide: the mechanisms of oxidation and exfoliation. J Mater Sci 47:4400–4409
38. Ruoff R (2008) Graphene: Calling all chemists. Nat Nanotechnol 3:10–11
39. Jiang H (2011) Chemical preparation of graphene-based nanomaterials and their applications in chemical and biological sensors. Small 7:2413–2427
40. Mombeshora E, Ndungu P, Nyamori V (2017) Effect of graphite/sodium nitrate ratio and reaction time on the physicochemical properties of graphene oxide. New Carbon Mater 32:174–187
41. Ahmed M, Giwa A, Hasan S (2019) Chapter 26—Challenges and opportunities of graphene-based materials in current desalination and water purification technologies. Nanoscale Mater Water Purific Micro Nano Technol, pp 735–758
42. Sitko R, Turek E, Zawisza B, Malicka E, Talik E, Heimann J, Gagor A, Feist B, Wrzalik R (2013) Adsorption of divalent metal ions from aqueous solutions using graphene oxide. Dalton Trans 42:5682–5689
43. Atieh M, Bakather O, Tawabini B, Bukhari A, Khaled M, Alharthi M, Fettouhi M, Abuilaiwi F (2010) Removal of chromium(III) from water by using modified and nonmodified carbon nanotubes. J Nanomater 2010:17–30
44. Machida M, Mochimaru T, Tatsumoto H (2006) Lead(II) adsorption onto the graphene layer of carbonaceous materials in aqueous solution. Carbon 44:2681–2688
45. Lerf A, Buchsteiner A, Pieper J, Schöttl S, Dekany I, Szabo T, Boehm H (2006) Hydration behavior and dynamics of water molecules in graphite oxide. J Phys Chem Solids 67:1106–1110
46. Hummers WS, Offeman RE (1958) Preparation of graphitic oxide. J Am Chem Soc 80(6):1339
47. Stankovich S, Dikin DA, Piner RD, Kohlhaas KA, Kleinhammes A, Jia Y, Wu Y, Nguyen ST, Ruoff RS (2007) Synthesis of graphene-based nanosheets via chemical reduction of exfoliated graphite oxide. Carbon 45(7): 1558e1565
48. Alamgir A (2017) Drugs: their natural, synthetic, and biosynthetic sources. Therapeutic Use Med Plants Extracts 1(2017):105–123
49. Simazaki D, Kubota R, Suzuki T, Akiba M, Nishimura T, Kunikane S (2015) Occurrence of selected pharmaceuticals at drinking water purification plants in Japan and implications for human health. Water Res 76:187–200
50. Multinational Corporations Including Merck, Hoffman-La Roche, Burroughs-Wellcome (Now Part Of Glaxo Smith Kline), Abbott Laboratories, Eli Lilly And Upjohn (Now Part Of Pfizer) Began As Local Apothecary Shops In The Mid-1800s
51. Top pharmaceuticals: introduction: emergence of pharmaceutical science and industry, pp 1870–1930 (2022)
52. FDA (2017) Orange book: approved drug products with therapeutic equivalence. US Food & Drug Administration, USA
53. OECD (2017) Health at a glance 15. OECD Publishing, Paris
54. Gavrilescu M, Demnerova K, Aamand J, Agathos S, Fava F (2015) Emerging pollutants in the environment: present and future challenges in biomonitoring, ecological risks and bioremediation. N Biotechnol 32:147e156
55. Petrie B, Barden R, Kasprzyk-Hordern B (2015) A review on emerging contaminants in wastewaters and the environment: current knowledge, understudied areas and recommendations for future monitoring. Water Res 72:3e27
56. Voogt PD, Janex-Habibi M-L, Sacher F, Puijker L, Mons M (2009) Development of an international priority list of pharmaceuticals relevant for the water cycle. Water Sci Technol 59:39e46
57. Barbosa MO, Moreira NF, Ribeiro AR, Pereira MF, Silva AM (2016) Occurrence and removal of organic micropollutants: an overview of the watch list of EU Decision 2015/495. Water Res 94:257e279
58. Luo Y, Guo W, Ngo HH, Nghiem LD, Hai FI, Zhang J, Liang S, Wang XC (2014b) A review on the occurrence of micropollutants in the aquatic environment and their fate and removal during wastewater treatment. Sci Total Environ 1473:619e641
59. OECD Studies on water (2019) Pharmaceutical residues in freshwater: Hazards and policy responses. https://doi.org/10.1787/22245081
60. Patil A, Maiti S, Mallick A, Kulkarni K, Adivarekar R (2020) Cationization as Tool for Functionalization of Cotton. Adv Function Finish Textiles, pp 289–311
61. Gupta V, Suhas AI, Saini V (2004) Removal of rhodamine B, fast green, and methylene blue from wastewater using red mud, an aluminum industry waste. Ind Eng Chem Res 43:1740–1747
62. Bhattacharya S, Shunmugam R (2020) Polymer based gels and their applications in remediation of dyes from textile effluents. J Macromol Sci Part A 57:12
63. Elwakeel K (2009) Removal of Reactive Black 5 from aqueous solutions using magnetic chitosan resins. J Hazard Mater 167:383–392
64. Azari A, Nabizadeh R, Nasseri S, Mahvi AH, Mesdaghinia AR (2020) Comprehensive systematic review and meta-analysis of dyes adsorption by carbon-based adsorbent materials: Classification and analysis of last decade studies. Chemosphere 250:126238
65. Reddy S, Kotaiah B, Reddy N, Velu M (2006) The removal of composite reactive dye from dyeing unit effluent using sewage sludge derived activated carbon. Turk J Eng Environ Sci 30:367–373
66. Chung K-T (2016) Azo dyes and human health: a review. J Environ Sci Health, Part C 34:233–261
67. Solis M, Solis A, Perez H, Manjarrez N, Flores M (2012) Microbial decolouration of azo dyes: a review. Process Biochem 47:1723–1748
68. Jayanthy V, Geetha R, Rajendran R, Prabhavathi P, Sundaram K, Kumar D, Santhanam P (2014) Phytoremediation of dye contaminated soil by Leucaena leucocephala (subabul) seed and growth assessment of Vigna radiata in the remediated soil. Saudi J Biol Sci 21:324–333
69. Imran M, Shaharoona B, Crowley D, Khalid A, Hussain S, Arshad M (2015) The stability of textile azo dyes in soil and their impact on microbial phospholipid fatty acid profiles. Ecotoxicol Environ Saf 120:163–168
70. Siddiqui SI, Rathi G, Chaudhry SA (2018) Acid washed black cumin seed powder preparation for adsorption of methylene blue dye from aqueous solution: thermodynamic, kinetic and isotherm studies. J Mol Liq 264:275–284
71. Saranraj P (2013) Bacterial biodegradation and decolourization of toxic textile azo dyes. Afr J Microbiol Res 7(30):3885–3890
72. Forgacs E, Cserh´ati T, Oros G, (2004) Removal of synthetic dyes from wastewaters: a review. Environ Int 30(7):953–971
73. Slama HB, Bouket AC, Pourhassan Z, Alenezi FN, Silini A, Cherif-Silini H, Oszako T, Luptakova L, Goli'nska P, Belbahri L, (2021) Diversity of synthetic dyes from textile industries, discharge impacts and treatment methods. Appl Sci 11:6255
74. Sharma J, Sharma S, Soni V (2021) Classification and impact of synthetic textile dyes on aquatic flora: a review. Re Stud Mar Sci 45:101802
75. Yamjala K, Nainar M, Ramisetti N (2016) Methods for the analysis of azo dyes employed in food industry–a review. Food Chem 192:813–824
76. Benkhaya S, M'rabet S, El Harfi A (2020) A review on classifications, recent synthesis and applications of textile dyes. Inorg Chem Commun 115:107891

77. Jain K, Madamwar D, Tiwari O (2019) Mapping of research outcome on remediation of dyes. Dye intermediates and textile industrial waste
78. Shakoor S, Nasar A (2016) Removal of methylene blue dye from artificially contaminated water using citrus limetta peel waste as a very low cost adsorbent. J Taiwan Inst Chem Eng 66:154–163
79. Xiao H, Zhao T, Li C, Li M (2017) Eco-friendly approaches for dyeing multiple type of fabrics with cationic reactive dyes. J Cleaner Prod 165:1499–1507
80. Jalandoni-Buan A, Decena-Soliven A, Cao E, Barraquio V, Barraquio W (2010) Characterization and identification of Congo red decolorizing bacteria from monocultures and consortia. Philipp J Sci 139:71–78
81. Sponza D, Isik M (2005) Toxicity and intermediates of CI Direct Red 28 dye through sequential anaerobic/aerobic treatment. Proc Biochem 40:2735–2744
82. Burkinshaw S, Son Y-A (2010) The dyeing of supermicrofibre nylon with acid and vat dyes. Dyes Pigm 87:132–138
83. Anyahara JN (2021) Effects of polycyclic aromatic hydrocarbons (PAHs) on the environment: a systematic review. Int J Adv Acad Res 7:2488–9849
84. Singh PK, Singh RP, Singh P, Singh RL (2019) Food hazards: physical, chemical, and biological. Food Safety Human Health, pp 15–65
85. Hiew BYZ, Lee LY, Lee XJ, Thangalazhy-Gopakumar S, Gan S, Lim SS, Pan G-T, Yang TC-K, Chiu WS, Khiew PS (2018) Review on synthesis of 3D graphene-based configurations and their adsorption performance for hazardous water pollutants. Proc Saf Environ Prot 116:262–286
86. Awad AM, Jalab R, Benamor A, Nasser MS, Ba-Abbad MM, El-Naas M, Mohammad AW (2020) Adsorption of organic pollutants by nanomaterial-based adsorbents: an overview. J Mol Liq 301:112335
87. Yang J, Shojaei S, Shojaei S (2022) Removal of drug and dye from aqueous solutions by graphene oxide: Adsorption studies and chemometrics methods. npj Clean Water (2022) 5:5
88. Foroutan R, Mohammadi R, MousaKhanloo F, Sahebi S, Ramavandi B, Kumar PS, Vardhan KH (2020) Performance of montmorillonite/graphene oxide/$CoFe_2O_4$ as a magnetic and recyclable nano-composite for cleaning methyl violet dye-laden wastewater. Adv Powder Technol 31:3993–4004
89. Feng X, Qiu B, Dang Y, Sun D (2021) Enhanced adsorption of naproxen from aquatic environments by β-cyclodextrin-immobilized reduced graphene oxide. Chem Eng J 412:128710
90. Jaswal A, Kaur M, Singh S, Kansal SK, Umar A, Garoufalis CS, Baskoutas S (2021) Adsorptive removal of antibiotic ofloxacin in aqueous phase using rGO-MoS_2 heterostructure. J Hazard Mater 417:125982
91. Akpotu SO, Moodley B (2018) MCM-48 encapsulated with reduced graphene oxide/graphene oxide and as-synthesised MCM-48 application in remediation of pharmaceuticals from aqueous system. J Mol Liq 261:540–549
92. Ogunleye T, Akpotu SO, Moodley B (2020) Adsorption of sulfamethoxazole and reactive blue 19 using graphene oxide modified with imidazolium based ionic liquid. Environ Technol Innovation 17:100616
93. Suna Y, Chena M, Liua H, Zhub Y, Wanga D, Yan M (2020) Adsorptive removal of dye and antibiotic from water with functionalized zirconium-based metal organic framework and graphene oxide composite nanomaterial Uio-66-$(OH)_2$/GO. Appl Surf Sci 525:146614
94. Wang G, Li G, Huan Y, Hao C, Chen W (2020) Acrylic acid functionalized graphene oxide: High-efficient removal of cationic dyes from wastewater and exploration on adsorption mechanism. Chemosphere 261:127736
95. Jiang X, Pan W, Xiong Z, Zhang Y, Zhao L (2021) Facile synthesis of layer-by-layer decorated graphene oxide based magnetic nano-composites for β-agonists/dyes adsorption removal and bacterial inactivation in wastewater. J Alloys Compd 870:159414
96. Tran TV, Vo DVN, Nguyen DTC, Ching YC, Nguyen NT, Nguyen QT (2022) Effective mitigation of single-component and mixed textile dyes from aqueous media using recyclable graphene-based nano-composite. Environ Sci Pollut Res 29:32120–32141
97. Geim AK, Novoselov KS (2007) The rise of graphene. Nat Mater 6:183–191
98. Brumfiel G (2009) Graphene gets ready for the big time. Nat 458:390–391
99. Li D, Kaner RB (2008) Graphene-based materials. Science 320(5880):1170–1171
100. Park S, Ruoff RS (2009) Chemical methods for the production of graphenes. Nat Nanotechnol 4:217–224
101. Novoselov K, Geim AK, Morozov S, Jiang D, Katsnelson M, Grigorieva I, Dubonos S, Firsov A (2005) Two-dimensional gas of massless Dirac fermions in graphene. Nature 438:197–200
102. Zhang Y, Tan YW, Stormer HL, Kim P (2005) Experimental observation of the quantum Hall effect and Berry's phase in graphene. Nat 438:201–204
103. Lee C, Wei X, Kysar JW, Hone J (2008) Measurement of the elastic properties and intrinsic strength of monolayer graphene. Science 321:385–388
104. Bolotin KI, Sikes K, Jiang Z, Klima M, Fudenberg G, Hone J, Kim P, Stormer H (2008) Ultrahigh electron mobility in suspended graphene. Solid State Commun 146:351–355
105. Dreyer DR, Park S, Bielawski CW, Ruoff RS (2010) The chemistry of graphene oxide. Chem Soc Rev 39:228–240
106. Niyogi S, Bekyarova E, Itkis ME, McWilliams JL, Hamon MA, Haddon RC (2006) Solution properties of graphite and graphene. J Am Chem Soc 128:7720–7721
107. Liu ZB, Xu YF, Zhang XY, Zhang XL, Chen YS, Tian JG (2009) Porphyrin and fullerene covalently functionalized graphene hybrid materials with large nonlinear optical properties. J Phys Chem B 113:9681–9686
108. Liu Z, Robinson JT, Sun X, Dai H (2008) PEGylated nanographene oxide for delivery of water-insoluble cancer drugs. J Am Chem Soc 130:10876–10877
109. Veca LM, Lu F, Meziani MJ, Cao L, Zhang P, Qi G, Qu L, Shrestha M, Sun YP (2009) Polymer functionalization and solubilization of carbon nanosheets. Chem Commun 14(18):2565–2567
110. Wang S, Chia PJ, Chua LL, Zhao LH, Png RQ, Sivaramakrishnan S, Zhou M, Goh RG, Friend RH, Wee AT (2008) Band-like transport in surface-functionalized highly solution-processable graphene nanosheets. Adv Mater 20:3440–3446
111. Yang H, Shan C, Li F, Han D, Zhang Q, Niu L (2009) Covalent functionalization of polydisperse chemically-converted graphene sheets with amine-terminated ionic liquid. Chem Commun 26:3880–3882
112. Yang H, Li F, Shan C, Han D, Zhang Q, Niu L, Ivaska A (2009) Covalent functionalization of chemically converted graphene sheets via silane and its reinforcement. J Mater Chem 19:4632–4638
113. Hou S, Su S, Kasner ML, Shah P, Patel K, Madarang CJ (2010) Formation of highly stable dispersions of silane-functionalized reduced graphene oxide. Chem Phys Lett 501:68–74
114. Yang X, Zhang X, Liu Z, Ma Y, Huang Y, Chen Y (2008) High-efficiency loading and controlled release of doxorubicin hydrochloride on graphene oxide. J Phys Chem C 112:17554–17558
115. Lu CH, Yang HH, Zhu CL, Chen X, Chen GN (2009) A graphene platform for sensing biomolecules. Angew Chem 121:4879–4881

116. Hao L, Wang X, Huang Q, Liu M, Zhang C, Chen J, Zhang P, Cai X (2017) One step green reduced and functionalized graphene oxide for highly efficient loading and effectively release of doxorubicin hydrochloride. J Biomed Nanotechnol 13:1309–1320
117. Karanfil T, Dastgheib SA (2004) Trichloroethylene adsorption by fibrous and granular activated carbons: aqueous phase, gas phase, and water vapor adsorption studies. Environ Sci Technol 38:5834–5841
118. Bandosz T (2006) Desulfurization on activated carbons. Interface Sci Technol 7:231–292
119. Karanfil T, Kilduff JE (1999) Role of granular activated carbon surface chemistry on the adsorption of organic compounds. 1. Priority pollutants Environ Sci Technol 33:3217–3224
120. Pignatello JJ, Xing B (1995) Mechanisms of slow sorption of organic chemicals to natural particles. Environ Sci Technol 30:1–11
121. Olanipekun O, Oyefusi A, Neelgund GM, Oki A (2014) Adsorption of lead over graphite oxide. Spectrochimica Acta A 118:857–860
122. Mowla, D, Do, D. D, Kaneko, K (2003) Adsorption of water vapor in activated carbon: a brief review. Chem Phys Carbon. Radovic, L. R., Ed.; Marcel Dekker, New York, 28:229–262
123. Rápó E, Posta K, Suciu M, Szép R, Tonk S (2019) Adsorptive removal of remazol brilliant violet-5R dye from aqueous solutions using calcined eggshell as biosorbent. Acta Chim Slov 66:648–658
124. Brito MJ, Veloso CM, Santos LS, Bonomo RC, Fontan RD (2018) Adsorption of the textile dye dianix® royal blue cc onto carbons obtained from yellow mombin fruit stones and activated with KOH and H_3PO4: KINETICS, ADSORPTION EQUILIBRIUM AND THERMODYNAMIC studies. Powder Technol 339:334–343
125. Gamoudi S, Srasra E (2019) Adsorption of organic dyes by HDPy+-modified clay: effect of molecular structure on the adsorption. J Mol Struct 1193:522–531
126. Kanwal A, Bhatti HN, Iqbal M, Noreen S (2017) Basic dye adsorption onto clay/$MnFe_2O_4$ composite: a mechanistic study. Water Environ Res 89:301–311
127. Yildirim A (2021) Removal of the anionic dye reactive orange 16 by chitosan/tripolyphosphate/mushroom. Chem Eng Technol 44:1371–1381
128. Khasri A, Jamir MRM, Ahmad AA, Ahmad MA (2021) Adsorption of Remazol Brilliant Violet 5R Dye from aqueous solution onto Melunak and Rubberwood Sawdust based activated carbon: interaction mechanism, isotherm, kinetic and thermodynamic properties. DWT 216:401–411
129. Liu J, Liu G, Liu W (2014) Preparation of water-soluble b-cyclodextrin/poly(acrylic acid)/graphene oxide nano-composites as new adsorbents to remove cationic dyes from aqueous solutions. Chem Eng J 257:299–308
130. Fu C, Dong X, Wang S, Kong F (2019) Synthesis of nano-composites using xylan and graphite oxide for remediation of cationic dyes in aqueous solutions. Int J Biol Macromol 137:886–894
131. Mahmoodi NM, Oveisi M, Bakhtiari M, Hayati B, Shekarchi AA, Bagheri A, Rahimi S (2019) Environmentally friendly ultrasound-assisted synthesis of magnetic zeolitic imidazolate framework—Graphene oxide nano-composites and pollutant removal from water. J Mol Liq 282:115–130
132. Mahmoodi NM, Oveisi M, Asadi E (2019) Synthesis of NENU metal-organic framework-graphene oxide nano-composites and their pollutant removal ability from water using ultrasound. J Cleaner Prod 211:198–212
133. Farghali MA, Abo-Aly MM, Salaheldin TA (2021) Modified mesoporous zeolite-A/reduced graphene oxide nano-composite for dual removal of methylene blue and Pb^{2+} ions from wastewater. Inorg Chem Commun 126:108487
134. Ninwiwek N, Hongsawat P, Punyapalakul P, Prarat P (2019) Removal of the antibiotic sulfamethoxazole from environmental water by mesoporous silica-magnetic graphene oxide nanocomposite technology: adsorption characteristics, coadsorption and uptake mechanism. Colloids Surf A 580:123716
135. Nodeh MKM, Radfard M, Zardari LA, Nodeh HR (2018) Enhanced removal of naproxen from wastewater using silica magnetic nanoparticles decorated onto graphene oxide; parametric and equilibrium study. Sep Sci Technol 53(15):2476–2485
136. Karimi-Maleh H, Shafieizadeh M, Taher MA, Opoku F, Kiarii EM, Govender PP, Ranjbari S, Rezapour M, Orooji Y (2019) The role of magnetite/graphene oxide nano-composite as a high efficiency adsorbent for removal of phenazopyridine residues from water samples, an experimental/theoretical investigation. J Mol Liq 298:1120240
137. Kyzas GZ, Bikiaris DN, Seredych M, Bandosz TJ, Deliyanni EA (2014) Removal of dorzolamide from biomedical wastewaters with adsorption onto graphite oxide/poly(acrylic acid) grafted chitosan nano-composite. Bioresour Technol 152:399–406
138. Li C-M, Chen C-H, Chen W-H (2016) Chen W-H (2017) Different influences of nanopore dimension and pH between chlorpheniramine adsorptions on graphene oxide-iron oxide suspension and particle. Chem Eng J 307:447–455
139. Yeow PK, Wong SW, Hadibarata T (2020) Removal of azo and anthraquinone dye by plant biomass as adsorbent—a review. Biointerface Res Appl Chem 11:8218–8232
140. Badawy AA, Ibrahim SM, Essawy HA (2020) Enhancing the textile dye removal from aqueous solution using cobalt ferrite nanoparticles prepared in presence of fulvic acid. J Inorg Organomet Polym 30:1798–1813
141. Szende T, Eszter R (2020) Környezeti Szennyez˝ok, Környezeti Problémák, Környezeti Remediáció, 1st ed.; EXIT Kiadó: Cluj Napoca, Romania. ISBN 978–606–9091–23–4.
142. Abualnaja KM, Alprol AE, Abu-Saied MA, Ashour M, Mansour AT (2021) Removing of anionic dye from aqueous solutions by adsorption using of multiwalled carbon nanotubes and poly(acrylonitrile-styrene) impregnated with activated carbon. Sustainability 13:7077
143. Khalaf IH, Al-Sudani FT, AbdulRazak AA, Aldahri T, Rohani S (2021) Optimization of congo red dye adsorption from wastewater by a modified commercial zeolite catalyst using response surface modeling approach. Water Sci Technol 83:1369–1383
144. Sharma K, Sharma S, Sharma V, Mishra PK, Ekielski A, Sharma V, Kumar V (2021) Methylene blue dye adsorption from wastewater using hydroxyapatite/gold nano-composite: kinetic and thermodynamics studies. Nanomater 11:1403
145. Hosseinzadeh H, Ramin S (2017) Fabrication of starch-graft-poly(acrylamide)/graphene oxide/hydroxyapatite nano-composite hydrogel adsorbent for removal of malachite green dye from aqueous solution. Int J Biol Macromol 106:101–115
146. Huang T, Yan M, Kai He, Huang Z, Zeng G, Chen A, Peng M, Li H, Yuan L, Chen G (2019) Efficient removal of methylene blue from aqueous solutions using magnetic graphene oxide modified zeolite. J Colloid Interf Sci 543:43–51
147. Konicki W, Aleksandrzak M, Moszyński D, Mijowska E (2017) Adsorption of anionic azo-dyes from aqueous solutions onto graphene oxide: equilibrium, kinetic and thermodynamic studies. J Colloid Interf Sci 496:188–200
148. Jinendra U, Bilehal D, Nagabhushana BM, Kumar AP (2021) Adsorptive removal of Rhodamine B dye from aqueous solution by using graphene–based nickel nano-composite. Heliyon 7:e06851

149. Othman NH, Alias NH, Shahruddin MZ, Bakar NFA, Him NRN, Lau WJ (2018) Adsorption kinetics of methylene blue dyes onto magnetic graphene oxide. Environ Chem Eng 6:2803–2811
150. Kerkez-Kuyumcu O¸ Bayazit S, Salam MA, (2016) Antibiotic amoxicillin removal from aqueous solution using 3 magnetically modified graphene nanoplatelets. J Ind Eng Chem 36:198–205
151. Delhiraja K, Vellingiri K, Boukhvalov DW, Philip L (2019) Development of highly water stable graphene oxide-based composites for the removal of pharmaceuticals and personal care products. Ind Eng Chem Res 58:2899–2913
152. Ma J, Sun Y, Yu F (2017) Efficient removal of tetracycline with KOH-activated graphene from aqueous solution. Roy Soc Open Sci 4:170731
153. Nodeh MK, Soltani S, Shahabuddin S, Rashidi NH, Sereshti H (2018) Equilibrium, kinetic and thermodynamic study of magnetic polyaniline/graphene oxide based nano-composites for ciprofloxacin removal from water. J Inorg Organomet Polym 28:1226e1234
154. Miao J, Wang F, Chen Y, Zhu Y, Zhou Y, Zhang S (2019) The adsorption performance of tetracyclines on magnetic graphene oxide: a novel antibiotics absorbent. Appl Surf Sci 475:549–558
155. Li Z, Qi M, Tu C, Wang W, Chen J, Wang AJ (2017) Highly efficient removal of chlorotetracycline from aqueous solution using graphene oxide/TiO_2 composite: properties and mechanism. Appl Surf Sci 425:765–775
156. Yagub MT, Sen TK, Afroze S, Ang HM (2014) Dye and its removal from aqueous solution by adsorption: a review. Adv Colloid Interf Sci 209:172–184
157. Terangpi P, Chakraborty S (2017) Adsorption kinetics and equilibrium studies for removal of acid azo dyes by aniline formaldehyde condensate. Appl Water Sci 7:3661–3671
158. Hassani A, Çelikdağ G, Eghbali P, Sevim M, Karaca S, Metin Ö (2018) Heterogeneous sono-Fenton-like process using magnetic cobalt ferritereduced graphene oxide ($CoFe_2O_4$-rGO) nano-composite for the removal of organic dyes from aqueous solution. Ultrason-Sonochem 40:841–852
159. Shahabuddin S, Sarih NM, Kamboh MA, Nodeh HR, Mohamad S (2016) Synthesis of polyaniline-coated graphene oxide@srtio$_3$ nanocube nano-composites for enhanced removal of carcinogenic dyes from aqueous solution. Polymers 8:305
160. Rajabia M, Mahanpoora K, Moradi O (2019) Preparation of PMMA/GO and PMMA/GO-Fe_3O_4 nano-composites for malachite green dye adsorption: kinetic and thermodynamic studies. Composites B 167:544–555
161. Song Z, Ma Z-Y, Li C-E (2019) The residual tetracycline in pharmaceutical wastewater was effectively removed by using MnO_2/graphene nano-composite. Sci Total Environ 651:580–590
162. Šljivi´c-Ivanovi´C M, Smi˘ciklas I (2020) Utilization of C&D waste in radioactive waste treatment—Current knowledge and perspectives. In: Pacheco-Torgal F, Ding Y, Colangelo F, Tuladhar R, Koutamanis A, (eds) Advances in construction and demolition waste recycling. Woodhead Publishing Series in Civil and Structural Engineering; Woodhead Publishing: Sawaston, UK, Chapter 23, pp 475–500. ISBN 978–0–12–819055–5
163. Nikam S, Mandal D (2020) Experimental study of the effect of different parameters on the adsorption and desorption of trichloroethylene vapor on activated carbon particles. ACS Omega 5:28080–28087
164. Yang Q, Lu R, Ren SS, Chen C, Chen Z, Yang X (2018) Three dimensional reduced graphene oxide/ZIF-67 aerogel: effective removal cationic and anionic dyes from water. Chem Eng J 348:202–211
165. Sahraei R, Pour ZS, Ghaemy M (2017) Novel magnetic bio-sorbent hydrogel beads based on modified gum tragacanth/graphene oxide: Removal of heavy metals and dyes from water. J Clean Prod 142:2973–2984
166. Rong X, Qiu F, Qin J, Zhao H, Yan J, Yang D (2014) Facile hydrothermal synthesis, adsorption kinetics and isotherms to Congo Red azo-dye from aqueous solution of NiO/graphene nanosheets adsorbent. J Ind Eng Chem 26:354–363
167. Li MF, Liu YG, Zeng GM, Liu SB, Hu XJ, Shu D, Jiang LH, Tan XF, Cai XX, Yan ZL (2017) Tetracycline absorbed onto nitrilotriacetic acid-functionalized magnetic graphene oxide: influencing factors and uptake mechanism. J Colloid Interf Sci 485:269–279
168. Li MF, Liu YG, Liu SB, Zeng GM, Hu XJ, Tan XF, Jiang LH, Liu N, Wen J, Liu XH (2018) Performance of magnetic graphene oxide/diethylenetriaminepentaacetic acid nano-composite for the tetracycline and ciprofloxacin adsorption in single and binary systems. J Colloid Interf Sci 521:150–159
169. Ma J, Yang M, Yu F, Zheng J (2015) Water-enhanced removal of ciprofloxacin from water by porous graphene hydrogel. Sci Rep 5:13578
170. Tan F, Liu M, Ren S (2017) Preparation of polydopamine-coated graphene oxide/Fe_3O_4 imprinted nanoparticles for selective removal of fluoroquinolone antibiotics in water. Sci Rep 7:5735
171. Wang F, Yang B, Wang H, Song Q, Tan F, Cao Y (2016) Removal of ciprofloxacin from aqueous solution by a magnetic chitosan grafted graphene oxide composite. J Mol Liq 222:188–194
172. Zhuang S, Zhu X, Wang J (2018) Kinetic, equilibrium, and thermodynamic performance of sulfonamides adsorption onto graphene. Environ Sci Pollut Res 25:36615–36623
173. Rasheed T (2022) Magnetic nanomaterials: Greener and sustainable alternatives for the adsorption of hazardous environmental contaminants. J Clean Prod 362:132338
174. Carter MC, Weber WJ (1994) Modeling adsorption of TCE by activated carbon preloaded by background organic matter. Environ Sci Technol 28:614–623
175. Karanfil T, Kitis M, Kilduff J, Wigton A (1999) Role of granular activated carbon surface chemistry on the adsorption of organic compounds. 2. Natural organic matter Environ Sci Technol 33:3225–3233
176. Knappe DR, Snoeyink VL, Roche P, Prados MJ, Bourbigot M-M (1997) Atrazine removal by preloaded GAC. Water Resour 31(11):2899–2909
177. Mohanty K, Das D, Biswas MN Treatment of phenolic wastewater in a novel multi-stage external loop airlift reactor using activated carbon. Sep Purif Technol 58(3):311–319
178. Segovia-Sandoval SJ, Pastrana-Martínez LM, Ocampo-Pérez R, Morales-Torres S, Berber-Mendoza MS, Carrasco-Marín F (2019) Synthesis and characterization of carbon xerogel/graphene hybrids as adsorbents for metronidazole pharmaceutical removal: effect of operating parameters. Sep Purif Technol 237:116341
179. Chowdhury S, Balasubramanian R (2014) Recent advances in the use of graphene-family nanoadsorbents for removal of toxic pollutants from wastewater. Adv Colloid Interface Sci 204:35–56
180. Zheng Y, Cheng B, You W, Yu J, Ho W (2019) 3D hierarchical graphene oxide-NiFe LDH composite with enhanced adsorption affinity to Congo red, methyl orange and Cr (VI) ions. J Hazard Mater 369:214–225
181. Kern M, Škulj S, Rožman M (2022) Adsorption of a wide variety of antibiotics on graphene-based nanomaterials: A modelling study. Chemosphere 296:134010
182. Khalil AME, Han L, Maamoun I, Tabish TA, Chen Y, Eljamal O, Zhang S, Butler D, Memon FA (2022) Novel Graphene-Based Foam Composite As a Highly Reactive Filter Medium for the Efficient Removal of Gemfibrozil from (Waste)Water. Adv Sustain System 6(6):2200016
183. Liu Y, Men B, Hu A, You Q, Liao G, Wang D (2020) Facile synthesis of graphene-based hyper-crosslinked porous carbon

composite with superior adsorption capability for chlorophenols. J Environ Sci 90:395–407
184. Prarat P, Hongsawat P, Punyapalakul P (2020) Amino-functionalized mesoporous silica-magnetic graphene oxide nanocomposites as water-dispersible adsorbents for the removal of the oxytetracycline antibiotic from aqueous solutions: adsorption performance, effects of coexisting ions, and natural organic matter. Environ Sci Pollut Res Int 27:6560–6576
185. Li MF, Liu YG, Zeng GM, Liu SB, Hu XJ, Shu D, Jiang LH, Tan XF, Cai XX, Yan ZL (2017) Tetracycline absorbed onto nitrilotriacetic acid-functionalized magnetic graphene oxide: influencing factors and uptake mechanism. J Colloid Interface Sci 485:269–279
186. LiuY MB, Hu A, You Q, Liao G, Wang D (2020) Facile synthesis of graphene-based hyper-crosslinked porous carbon composite with superior adsorption capability for chlorophenols. J Environ Sci 90:395–407
187. Dutta S, Gupta B, Srivastava SK, Gupta AK (2021) Recent advances on the removal of dyes from wastewater using various adsorbents: a critical review. Mater Adv 2:4497–4531
188. Ho YS, Wang CC (2004) Pseudo-isotherms for the sorption of cadmium ion onto tree fern. Process Biochem 39:761–765
189. Kouyoumdjiev MS (1992) Kinetics of adsorption from liquid phase on activated carbon. Delft University
190. Kong Q, Wei C, Preis S, Hu Y, Wang F (2018) Facile preparation of nitrogen and sulfur co-doped graphene-based aerogel for simultaneous removal of Cd^{2+} and organic dyes. Environ Sci Pollut Res 25:21164–21175
191. Bharath G, Alhseinat E, Ponpandian N, Khan MA, Siddiqui MR, Ahmed F, Alsharaeh EH (2017) Development of adsorption and electrosorption techniques for removal of organic and inorganic pollutants from wastewater using novel magnetite/porous graphene-based nano-composites. Sep Purif Technol 188:206–218
192. Sharma P, Kaur H (2011) Sugarcane bagasse for the removal of erythrosin B and methylene blue from aqueous waste. Appl Water Sci 1:135–145
193. Chatzimarkou A, Stalikas C (2020) Adsorptive removal of estriol from water using graphene-based materials and their magnetite composites: Heterogeneous Fenton-like non-toxic degradation on magnetite/graphene oxide. Int J Environ Res 14:269–287
194. Menard D, Py X, Mazet N (2007) Activated carbon monolith of high thermal conductivity for adsorption processes improvement Part B. Thermal regeneration Chem Eng Process 46:565–572
195. Chiou M, Li H (2003) Adsorption behavior of reactive dye in aqueous solution on chemical cross-linked chitosan beads. Chemosphere 50:1095–1105
196. Nakano Y, Hua LQ, Nishijima W, Shoto E, Okada M (2000) Biodegradation of trichloroethylene (TCE) adsorbed on granular activated carbon (GAC). Water Res 34:4139–4142
197. Quan X, Liu X, Bo L, Chen S, Zhao Y, Cui X (2004) Regeneration of acid orange 7-exhausted granular activated carbons with microwave irradiation. Water Res 38:4484–4490
198. Lim JL, Okada M (2005) Regeneration of granular activated carbon using ultrasound. Ultrason Sonochem 12:277–282
199. Amari A, Elboughdiri N, Ghernaout D, Lajimi RH, Alshahrani AM, Tahoon MA, Rebah FB (2021) Multifunctional crosslinked chitosan/nitrogen-doped graphene quantum dot for wastewater treatment. Ain Shams Eng J 12(4):4007–4014
200. Zhu L-G, Liu S-B, Zeng G-M, Jiang L-H, Tan X-F, Zhou L, Zeng W, Li TT, Yang CP (2017) Adsorption of emerging contaminant metformin using graphene oxide. Chemosphere 179:20–28
201. Verma M, Tyagi I, Kumar V, Goel S, Vaya D, Kim H (2021) Fabrication of GO–MnO_2 nano-composite using hydrothermal process for cationic and anionic dyes adsorption: Kinetics, isotherm, and reusability. J Environ Chem Eng 9:106045
202. Kazeem TS, Zubair M, Daud M, Mu'azu ND, Al-Harthi MA, (2019) Graphene/ternary layered double hydroxide composites: Efficient removal of anionic dye from aqueous phase. Korean J Chem Eng 36(7):1057–1068
203. Jinendra U, Bilehal D, Nagabhushana BM, Kumar AP (221) Adsorptive removal of Rhodamine B dye from aqueous solution by using graphene–based nickel nano-composite. Heliyon 7:e06851
204. Gupta A, Viltres H, Gupta NK (2020) Sono-adsorption of organic dyes onto $CoFe_2O_4$/Graphene oxide Nano-composite. Surf Interf 20:100563
205. Das TR, Patra S, Madhuri R, Sharma PK (2017) Bismuth oxide decorated graphene oxide nano-composites synthesized via sonochemical assisted hydrothermal method for adsorption of cationic organic dyes. J Colloid Interface Sci 509:82–93
206. Soleimani K, Tehrani AD, Adeli M (2018) Bioconjugated graphene oxide hydrogel as an effective adsorbent for cationic dyes removal. Ecotoxico Environ Saf 147:34–42
207. Martins JT, Guimarães CH, Silva PM, Oliveira RL, Prediger P (2021) Enhanced removal of basic dye using carbon nitride/graphene oxide nano-composites as adsorbents: high performance, recycling, and mechanism. Environ Sci Pollut Res 28:3386–3405
208. Peng G, Zhang M, Deng S, Shan D, He Q, Yu G (2018) Adsorption and catalytic oxidation of pharmaceuticals by nitrogen-doped reduced graphene oxide/Fe_3O_4 nano-composite. Chem Eng J 341:361–370
209. Nodeh MKM, Soltani S, Shahabuddin S, Nodeh HR, Sereshti H (2018) Equilibrium, kinetic and thermodynamic study of magnetic polyaniline/graphene oxide based nano-composites for ciprofloxacin removal from water. J Inorg Organomet Polym Mater 28:1226–1234
210. Buekens A, Zyaykina N (2009) Adsorbents and adsorption processes for pollution control. Encyclopedia of Life Support Systems 2:1–10
211. Qu X, Alvarez PJ, Li Q (2013) Applications of nanotechnology in water and wastewater treatment. Water Res 47:3931–3946
212. Grant D, Skriba M, Saha AK (1987) Removal of radioactive contaminants from West Valley waste streams using natural zeolites. Environ Prog 6:104–109
213. Mier MV, Callejas RL, Gehr R, Cisneros BE, Alvarez PJ (2001) Heavy metal removal with mexican clinoptilolite: multi-component ionic exchange. Water Res 35:373–378
214. Gosset T, Trancart JL, Thévenot DR (1986) Batch metal removal by peat. Kinetics and thermodynamics Water Res 20:21–26
215. Mckay G (1995) Use of adsorbents for the removal of pollutants from wastewater. CRC Press
216. Crini G (2006) Non-conventional low-cost adsorbents for dye removal: a review. Bioresour Technol 97:1061–1085
217. Purkait MK, Maiti A, Dasgupta S, De S (2007) Removal of congo red using activated carbon and its regeneration. J Hazard Mater 145:287–295
218. Shamik C, Rajasekhar B (2014) Recent advances in the use of graphene-family nanoadsorbents for removal of toxic pollutants from wastewater. J Adv Colloid & Interface Sci 204:35–56
219. Huang Y, Chen X (2015) Carbon nanomaterial-based composites in wastewater purification. Nano Life 4:1–11